Journal of Environmental Management 150 (2015) 1–14

Contents lists available at ScienceDirect

Journal of Environmental Management

journal homepage: www.elsevier.com/locate/jenvman

Bioassessment of trace element contamination of Mediterranean coastal waters using the seagrass *Posidonia oceanica*

J. Richir [a, b, *], M. Salivas-Decaux [c], C. Lafabrie [c, d], C. Lopez y Royo [c], S. Gobert [a], G. Pergent [c], C. Pergent-Martini [c]

[a] Laboratory of Oceanology, MARE Centre, University of LIEGE, B6C, 4000 LIEGE, Sart Tilman, Belgium
[b] Institute of Marine Sciences, University of Portsmouth, Ferry Road, Portsmouth PO4 9LY, United Kingdom
[c] FRES 3041, EqEL, University of Corsica, Faculty of Sciences, BP 52, 20250 Corte, France
[d] UMR 241 EIO, University of French Polynesia, BP 6570, 98 702 Faa'a, Tahiti, French Polynesia

ARTICLE INFO

Article history:
Received 25 August 2014
Received in revised form
10 November 2014
Accepted 14 November 2014
Available online xxx

Keywords:
Mediterranean
Posidonia oceanica
Trace element (TE)
Water quality scale
Pollution index
Spatial analysis

ABSTRACT

A large scale survey of the trace element (TE) contamination of Mediterranean coastal waters was performed from the analysis of Ag, As, Cd, Cu, Hg, Ni and Pb in the bioindicator *Posidonia oceanica*, sampled at 110 sites differing by their levels of exposure to contaminants. The holistic approach developed in this study, based on the combined utilization of several complementary monitoring tools, *i.e.* water quality scale, pollution index and spatial analysis, accurately assessed the TE contamination rate of Mediterranean coastal waters. In particular, the mapping of the TE contamination according to a new proposed 5-level water quality scale precisely outlined the contamination severity along Mediterranean coasts and facilitated interregional comparisons. Finally, the reliability of the use of *P. oceanica* as bioindicator species was again demonstrated through several global, regional and local detailed case studies.

NB: The designations employed and the presentation of the information in this document do not imply the expression of any opinion whatsoever on the part of the authors concerning the legal status of any country, territory, city or area or of its authorities, or concerning the delimitation of its frontiers or boundaries.

1. Introduction

Because of the importance of coastal zones for human activities, a large percentage of the world population (41%; Martínez et al., 2007) and economic activities (61% of the gross world product; Agardy et al., 2005) are concentrated in a 100 km-wide strip along the coasts. With an estimated population of 132 million inhabitants that increases sharply during the summer tourist season, the Mediterranean coasts are particularly subject to strong human pressures (UNEP/MAP/Blue Plan, 2005; Durrieu de Madron et al., 2011). In 1996, the Mediterranean occupied the 7th place out of 35 in the list of the most threatened seas (UNEP/MAP, 1996) and was more recently presented as one of the world areas exhibiting the most serious environmental problems (UNEP/MAP/Blue Plan, 2005).

Human activities generate large volumes of waste that supply marine coastal environments in pathogens, organic matter, nutrients and toxicants (Durrieu de Madron et al., 2011). Among the wide range of toxicants are trace elements (TEs). The major anthropogenic emission sources of TEs result from mining and smelting activities (Callender, 2003); other important sources are linked to industrial, agricultural and urban activities that have been expanding in coastal zones since the early sixties (Bethoux et al., 1990; UNEP/MAP/Blue Plan, 2009). As TEs are toxic for aquatic organisms from threshold levels and as they are therefore likely to cause multiple damage to the population, the community and the ecosystem levels (Nordberg et al., 2007; Amiard, 2011), their environmental occurrence has to be accurately monitored in order to guarantee appropriate environmental management of coastal zones and to preserve marine coastal ecosystems and the goods and services they provide.

In this context, several European policies and directives related to coastal environment issues have emerged during these last years (Nobre, 2011). Among the most significant are the Water Framework Directive (WFD; EC, 2000), the Integrated Coastal Zone Management (ICZM) recommendation (EC, 2002) and the Marine Strategy Framework Directive (MSFD; EC, 2008). In parallel, regional (*e.g.* the National Strategy for ICZM of the Catalan Coast; Sardá et al., 2005) to transnational (*e.g.* the Convention for the

* Corresponding author. Laboratory of Oceanology, MARE Centre, University of LIEGE, B6C, 4000 LIEGE, Sart Tilman, Belgium. Tel.: +32 4366 3329; fax: +32 4366 5147.
E-mail address: jonathan.richir@alumni.ulg.ac.be (J. Richir).

http://dx.doi.org/10.1016/j.jenvman.2014.11.015
0301-4797/

Protection of the Marine Environment and the Coastal Region of the Mediterranean; UNEP/MAP, 2011) programs have been developed for the management of European marine environments. In addition, several initiatives aiming to identify sources and extent of water chemical contamination from the use of biological indicators have been developed in several Mediterranean coastal zones. Until recently, these initiatives have however mainly concerned the northwestern part of the Mediterranean.

Biological indicators (or bioindicators; Blandin, 1986) have the capacity to integrate the temporal changes of contaminants, concentrations or fluxes over various time-scales (Durrieu de Madron et al., 2011). Among the diversity of organisms used worldwide (Burger, 2006; Rainbow, 2006; Zhou et al., 2008), seagrasses (angiosperms) have been proposed as interesting bioindicators of water quality monitoring (Orth et al., 2006; Ralph et al., 2006; Lewis and Devereux, 2009). They indeed present several advantages in this regard: wide distribution worldwide (they occur in all the seas and oceans of the world with the exception of the Antarctic), integration of the global variations of the environment (at the sediment–water interface), responses to the environmental changes that are faster than those of organisms of higher trophic levels (at the basis of food webs), and facilitated detection of chemicals (high levels measured in their tissues: accumulator species; Phillips, 1994). As a consequence, angiosperms are regarded as one of the biological quality elements required for the assessment of ecological status of transitional and coastal waters (EC, 2000), and the more specific use of seagrasses as a well-suited tool for their ecological assessment has recently been highlighted in European water legislation (Foden and Brazier, 2007; Lopez y Royo et al., 2011).

In the Mediterranean, the long-lived perennial seagrass *Posidonia oceanica* (L.) Delile, that forms extensive monospecific meadows from sea level down to 25–45 m depth along almost the whole coastline (Procaccini et al., 2003; Gobert et al., 2006; Boudouresque et al., 2012), appears particularly interesting for water quality monitoring (Pergent-Martini et al., 2005; Montefalcone, 2009; Pergent et al., 2012). Its ability to accumulate TEs proportionally to environmental contamination levels has been clearly demonstrated through both field (Lafabrie et al., 2007a, 2009) and experimental (Warnau et al., 1996; Richir et al., 2013) approaches. Moreover, the interest of its use to assess the spatial and temporal extent of TE contaminations, at local and regional scales, has been frequently shown (Sanchiz et al., 2000; Ancora et al., 2004; Lafabrie et al., 2007b, 2008; Conti et al., 2010; Serrano et al., 2011; Copat et al., 2012; Luy et al., 2012; Cozza et al., 2013).

Thus, the objectives of the present study were (i) to assess, for the first time, the TE contamination in the entire Mediterranean biomonitored with *P. oceanica*, (ii) to propose a new 5-level water quality scale and (iii) to calculate coastal water pollution indices from bioaccumulated TE levels measured in that bioindicator, and (iv) to produce, on the basis of these data, accurate maps of the contamination of the Mediterranean by TEs. The overall aim of this work was thus to develop a holistic approach in order to provide scientists, stakeholders and decision makers with a global tool to bioassess the TE contamination severity of Mediterranean coastal waters. To achieve these objectives, 110 Mediterranean sites differing by their levels of exposure to contaminants, and 7 TEs (Ag, As, Cd, Cu, Hg, Ni and Pb) were considered.

2. Materials and methods

2.1. Sampling sites and sample processing

P. oceanica shoots were sampled at 10 ± 5 m depth by SCUBA diving at 110 sites located along the coasts of 13 Mediterranean countries (Fig. 1; Annex A). Sampling was carried out from 2003 to 2008, between April and July to minimize seasonal variations of TE concentrations (Capiomont et al., 2000). Sites were selected in order to cover the largest possible geographical distribution (according to local correspondents and scientific field sampling opportunities) and the widest range of anthropisation levels (according to known contamination sources). Only the blades of either the 2 external adult leaves or all the adult leaves, cleaned of their epiphytes, were considered for TE analysis (Lafabrie et al., 2008; Luy et al., 2012). Samples of 3–10 *P. oceanica* shoots were pooled into 3–5 replicates. Pooled samples were lyophilised (Heto® FD4-85, HetoHolten A/S; BenchTop 3L, VirTis Company Inc.) or sun dried at 25–35 °C to constant weight. They were then manually ground to powder.

2.2. Trace element analysis

Analyses included 7 TEs: silver (Ag), arsenic (As), cadmium (Cd), copper (Cu), mercury (Hg), nickel (Ni) and lead (Pb). Ag, As and Cu concentrations were assessed at 91 sites, Hg at 94 sites and Cd, Ni and Pb at all of the 110 sites.

Hg analyses were performed at the Laboratory EqEL of the University of Corte (Corsica, France), according to the method described in Lafabrie et al. (2007a). Briefly, samples were mineralized in Teflon digestion vessels, in a closed microwave digestion labstation (CEM® MARS 5, CEM Corporation), using nitric acid and hydrogen peroxide as reagents (normapur grade, Prolabo®). Analyses were performed by Cold Vapour Atomic Absorption Spectrometry (CV-AAS, PerkinElmer®).

Ag, As, Cd, Cu, Ni and Pb analyses were performed either at the Laboratory of Rouen/ETSA (COFRAC accredited laboratory, France) or at the Laboratory of Oceanology of the University of Liège (ULg, Belgium). At the Laboratory of Rouen/ETSA, analyses were performed by Graphite Furnace Atomic Absorption Spectrometry (GF-AAS) or Inductively Coupled Plasma Mass Spectrometry (ICP-MS), depending on the element analysed (no further information given). At the laboratory of Oceanology of the ULg, analyses were performed according to the method described in Richir et al. (2013). Briefly, samples were mineralized in Teflon digestion vessels, in a closed microwave digestion labstation (Ethos D, Milestone Inc.), using nitric acid and hydrogen peroxide as reagents (suprapur grade, Merck). Analyses were performed by Inductively Coupled Plasma Mass Spectrometry using Dynamic Reaction Cell technology (ICP-MS ELAN DRC II, PerkinElmer®).

The accuracy of analytical methods was checked using the certified reference material BCR 60 (*Lagarosiphon major*; $n = 3–11$; mean recovery = 103 ± 18%). TE concentrations are expressed in μg g_{DW}^{-1}. Ag concentrations that were found to be below their analytical detection limit (L_D) were considered as half of the L_D value during data statistical treatment.

2.3. Data processing

To compare global TE contamination levels among the 110 study sites, the Trace Element Pollution Index (TEPI) of Richir and Gobert (2014) was calculated, for each site, as follows:

$$TEPI = (Cf_1 * Cf_2 \cdots Cf_n)^{1/n},$$

where Cf_n is the mean normalized concentration of the TE n in a given monitored site. Not determined Ag, As, Cu and Hg concentrations were considered as their respective mean concentrations calculated from other available concentrations prior to TEPI calculation.

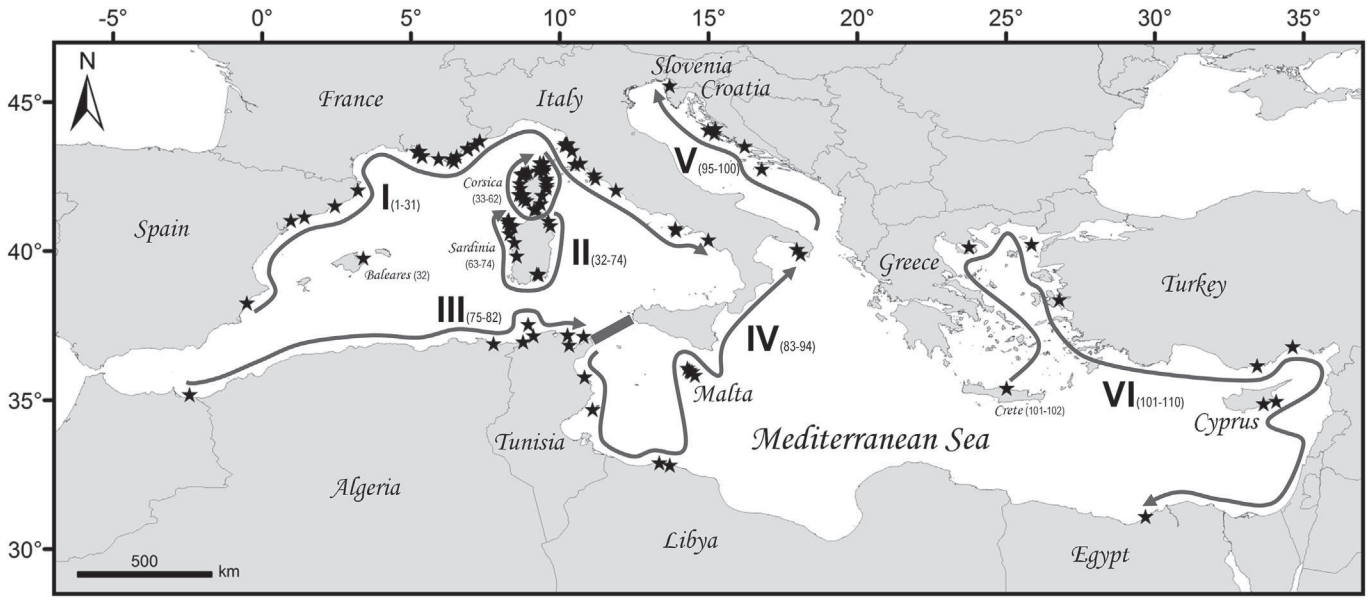

Fig. 1. Map showing the 110 sites located along the coasts of 13 Mediterranean countries and sampled for *Posidonia oceanica* between April and July of years 2003–2008. Stars represent sites; roman numbers and dark grey arrows represent the subdivision of the Mediterranean into 6 sub-areas, according to site location along its north-to-south and west-to-east axes. Sub-area I: 31 sites (1–31) along the European continental coasts (Spain–France–Italy); sub-area II: 43 sites (32–74) along the European insular coasts (Baleares, Spain–Corsica, France–Sardinia, Italy); sub-area III: 8 sites (75–82) along the North African coasts of the western Mediterranean (Spain–Algeria–Tunisia); sub-area IV: 12 sites (83–94) along the western coasts of the eastern Mediterranean (Tunisia–Lybia–Malta–Italy); sub-area V: 6 sites (95–100) along the Adriatic coasts (Croatia–Slovenia); sub-area VI: 10 sites (101–110) along the coasts of the Aegean-Levantine basin (Greece–Turkey–Cyprus–Egypt). For clarity purpose, site numbers and corresponding names were not reported on the map. Names of main European sampled islands (Baleares, Spain–Corsica, France–Sardinia, Italy–Crete, Greece) are also given. The thick dark grey line across the Strait of Sicily separates the western and the eastern Mediterranean basins. Because of the scale of the map, stars of many sites may overlap in whole or in part. Sites numbers and corresponding names together with their GPS coordinates are detailed in Annex A.

A new 5-level water quality scale was proposed using the quantile method. TE levels and TEPI values were ordered in ascending order prior quartile calculation. Data from each quartile were then averaged to determine class-limits of the scale. These are the 5 levels of the scale we propose: (1) the very low contamination level (VLCL, data below the 1st quartile mean), (2) the low contamination level (LCL, data between the 1st and 2nd quartile means), (3) the medium contamination level (MCL, data between the 2nd and 3rd quartile means), (4) the high contamination level (HCL, data between the 3rd and 4th quartile means), and (5) the very high contamination level (VHCL, data above the 4th quartile mean). Following classification, sites were GIS mapped according to their water quality level.

To order and to compare TEs according to the overall spatial variability of their environmental levels throughout the whole Mediterranean, the Trace Element Spatial Variation Index (TESVI) of Richir and Gobert (2014) was calculated, for each TE, as follows:

$$\mathrm{TESVI} = \left[\left(x_{\max}/x_{\min}\right)/\left(\sum(x_{\max}/x_i)/n\right)\right]{*}\mathrm{SD},$$

where x_{max} and x_{min} are the maximum and minimum mean concentrations recorded among the n sites, x_i are the mean concentrations recorded in each of the n sites, and SD is the standard deviation of the mean ratio $\sum(x_{max}/x_i)/n$.

2.4. Data statistical analysis

In this study, the Mediterranean was subdivided into 6 sub-areas according to site location along its north-to-south and west-to-east axes (Fig. 1; Annex A). In the western Mediterranean basin, 3 sub-areas were considered: (I) European continental coasts of Spain, France and Italy (sites 1–31); (II) European insular coasts of Baleares (Spain), Corsica (France) and Sardinia (Italy; sites 32–74); (III) North African coasts of Spain, Algeria and Tunisia (sites 75–82). In the eastern Mediterranean basin, 3 sub-areas were considered: (IV) western coasts of the eastern Mediterranean (Tunisia, Libya, Malta and Italy; sites 83–94); (V) Adriatic coasts of Croatia and Slovenia (sites 95–100); (VI) coasts of the Aegean-Levantine basin (Greece, Turkey, Cyprus and Egypt; sites 101–110).

Significant differences between sub-area mean TE concentrations and TEPI values were highlighted through one-way analysis of variance (one-way ANOVAs) followed by Tukey HSD pairwise comparison test of means with unequal n's ($p < 0.05$), after testing for normality and homogeneity of variances (Levene test) on raw or log-transformed data. Non-parametric analysis of variance (Kruskal–Wallis test) was performed when assumptions prior to ANOVAs (normality and/or homoscedasticity) were not achieved, followed by Dunn pairwise comparison test of means ($p < 0.05$).

Principal component analysis (PCA) and cluster analysis (CA) were performed on a data matrix with sampling sites as objects (rows) and Ag, As, Cd, Cu, Hg, Ni, Pb and TEPI as variables (columns). The half-range central value transformation was used as data pretreatment method (Moreda-Pineiro et al., 2001). Samples were clustered using Ward's method (Euclidean distance between objects as measure of similarity). In order to fulfil the data matrix prior PCA and CA, not determined Ag, As, Cu and Hg concentrations were considered as their respective mean concentrations calculated from other available concentrations. Following CA, sites were GIS mapped according to their belonging cluster.

Pearson's correlation coefficient was applied to identify correlations between TE concentrations and between TE concentrations and TEPI values, after testing for normality of distribution on raw or log-transformed data. When normality was not achieved, non-parametric Spearman's rank correlation coefficient was applied.

Statistical analyses were performed with STATISTICA 10 (StatSoft Inc.) and GraphPad Prism 5.03 (GraphPad Software Inc.) software. Maps were produced with ArcMap 10.2.1 (Esri Inc.).

3. Results

3.1. TE contamination range

Considering the 3 TEs (Cd, Ni and Pb) analysed in all 110 sampling sites (Figs. 2c,f,g; Annex A), St Raphaël (15; France) showed the maximum value for Cd (4.67 μg g_{DW}^{-1}), Canari (61; Corsica, France) the maximum value for Ni (123.0 μg g_{DW}^{-1}) and Porto Ercole (27; Italy) the maximum value for Pb (14.50 μg g_{DW}^{-1}). In contrast, Monastir (83; Tunisia) showed the minimum value for Cd (0.37 μg g_{DW}^{-1}) and Ni (1.6 μg g_{DW}^{-1}) and Macinaggio (33; Corsica, France) the minimum value for Pb (0.60 μg g_{DW}^{-1}). Cd mean levels were lower in sub-areas III to V while Ni and Pb mean levels, respectively lower in sub-areas III, IV, VI and II, V, VI were higher in sub-area I (Table 1; Annex B); these differences were not significant ($p > 0.05$).

For Hg analysed in 94 of the 110 sampling sites (Fig. 2e; Annex A), Urla (105; Turkey) showed the maximum value (0.2041 μg g_{DW}^{-1}), while the minimum value was reported for the Calvi fishfarm site (56; Corsica, France; 0.0200 μg g_{DW}^{-1}). Hg mean levels did not significantly ($p > 0.05$) differ between sub-areas, although slightly higher in sub-areas I and VI (Table 1; Annex B).

For the 3 remaining TEs (Ag, As and Cu) analysed in 91 of the 110 sampling sites (Figs. 2a,b,d; Annex A), Ile Rousse (59; Corsica, France) showed the maximum value for Ag (1.550 μg g_{DW}^{-1}), Brbinjscica (98; Croatia) the maximum value for As (5.300 μg g_{DW}^{-1}) and Olbia (63; Sardinia) the maximum value for Cu (27.70 μg g_{DW}^{-1}). Of the 14 sites with Ag levels below the 0.100 μg g_{DW}^{-1} L_D value, 9 were located in the Aegean-Levantine basin (sub-area VI). The minimum value for As (0.133 μg g_{DW}^{-1}) was recorded in St Paul's Bay (89; Malta) and the minimum value for Cu (1.87 μg g_{DW}^{-1}) at Monastir (83; Tunisia). Ag, As and Cu mean levels significantly differed ($p < 0.05$) between western and eastern Mediterranean sub-basins, with higher Ag and Cu mean levels in sub-area I compared to sub-areas IV (Ag, Cu) and VI (Ag) and higher As mean level in sub-area I compared to sub-areas II, IV and VI (Table 1; Annex B).

Based on TEPI values, La Vesse (7; France) was the most contaminated site (high Ag, As, Cu, Ni and Pb mean levels) and Monastir (83; Tunisia) the least contaminated (minimum Cd, Cu and Ni mean levels; Fig. 2h; Annex A). In the western Mediterranean, European continental coasts (sub-area I) were more contaminated than insular coasts (sub-area II; significant, $p < 0.05$) and North African coasts (sub-area III; not significant, $p > 0.05$). Overall, TE contamination was lower in the eastern Mediterranean (sub-areas IV and VI) compared to the western Mediterranean (sub-area I; significant, $p < 0.05$; sub-areas II and III; not significant, $p > 0.05$), except in the Adriatic (sub-area V; Table 1; Annex B).

3.2. Spatial distribution of TE contamination

According to the new proposed coastal water quality scale (Table 2), sites highly to very highly contaminated by Cd were indistinctly distributed along the continental and insular coasts of the entire Mediterranean, with however a predominance along the European coasts of the western Mediterranean. Accordingly, sites very little contaminated by Cd were found indistinctly in the entire Mediterranean (Fig. 2c; Table 2; Annex C). All sites highly to very highly contaminated by Ni were located along the French and Italian continental coasts, along the Corsican coast and in the Adriatic, except for Porto-Torres 3 (71; Sardinia, Italy), Salammbó (81; Tunisia) and Gokceada (104; Turkey). Conversely, sites very little contaminated by Ni were found along the North African coasts, in Crete (Ligaria, 102; Greece) and Turkey (Urla, 105), except for the 3 Italian sites Porto Ercole (27), Oristano (67) and Bosa (68; Fig. 2f; Table 2; Annex C). Sites highly to very highly contaminated by Pb were distributed along continental and insular coasts of the western Mediterranean and along the Maltese coasts, except for Ligaria (102; Crete, Greece) and Gokceada (104; Turkey). All sites of the western Mediterranean very little contaminated by Pb except Santa Marinella (28; Italian continental coast) were found along the insular coasts of Corsica (France) and Sardinia (Italy). Sites very little contaminated by Pb were proportionally more abundant in the eastern Mediterranean and evenly distributed (Fig. 2g; Table 2; Annex C).

Sites highly to very highly contaminated by Hg were proportionally very abundant in the Aegean-Levantine basin and along the French and northern Italian continental coasts. Hg contaminated sites were also found along the North African coasts, from Tunisia to Libya, along Maltese coasts and in the Adriatic, and sporadically distributed along Corsican (France), Sardinian (Italy) and Spanish European coasts. Three of the sites very little contaminated by Hg were found in Corsica (France), in addition to Chafarinas (75; Spain), Monastir (83; Tunisia), Brbinjscica (98; Croatia) and Kalogria (103; Greece; Fig. 2e; Table 2; Annex C).

With the exception of Salammbó (81; Tunisia) and Zadar (99; Croatia), all sites highly to very highly contaminated by Ag were located along the European continental coasts of the western Mediterranean and to a lesser extent along the insular coasts of Corsica (France) and Sardinia (Italy). Conversely, most sites very little contaminated by Ag were located in the Aegean-Levantine basin (Fig. 2a; Table 2; Annex C). The French continental coast was particularly contaminated by As, as were the 2 Croatian sites of Lavdara (97) and mainly Brbinjscica (98). Isolated cases of high to very high As contaminations were also recorded along the coasts of Spain, Italy (continental and Sardinian coasts), Corsica (France), Tunisia and Turkey. Conversely, Malta was very little contaminated by As, as were several sites distributed along the insular coasts of Corsica (France), Sardinia (Italy), Crete (Greece) and Cyprus (Fig. 2b; Table 2; Annex C). Most sites located along western European continental coasts were highly to very highly contaminated by Cu, as were half sites of the Adriatic and the 2 Cypriot sites. Isolated cases of high to very high Cu contamination were also recorded along the Corsican (France) and Sardinian (Italy) coasts. Except for one Turkish (Urla, 105) and two Sardinian sites (Cagliari 1, 66, and Oristano, 67; Italy), all sites very little contaminated by Cu were found along the Tunisian, Libyan and Maltese coasts (Fig. 2d; Table 2; Annex C).

Regarding the global contamination by the 7 studied TEs (*i.e.* TEPI values), 74% of sites located along the European continental coasts of the western Mediterranean were highly to very highly contaminated, against 35% of sites along its insular coasts. Except for Salammbó (81; Tunisia) and Brbinjscica (98; Croatia), no highly to very highly contaminated sites were found along the North African coasts of the western Mediterranean or in the eastern Mediterranean. Accordingly, all sites globally very little contaminated were found in the eastern Mediterranean, Adriatic Sea excluded, except for Oristano (67; Sardinia, Italy) and Chafarinas (75; Spain; Figs. 2h,3; Table 2; Annex C).

Regarding the overall spatial variability of the 7 studied TE coastal levels throughout the whole Mediterranean (Table 3), Hg levels displayed the lowest variability, with a TESVI value of 3.9, followed by Cd (8.7), Cu (9.2) and Pb (13.3) levels. The overall spatial variability of As and Ag levels was intermediate, with respective TESVI values of 29.4 and 34.9, while Ni levels varied the most throughout the whole Mediterranean, with a TESVI value of 92.7 (the overall spatial variability of TE levels is graphically compared in Annex D).

3.3. Pattern recognition and correlations

65.9% of the total variance of the data set with TE concentrations and TEPI values was explained by the 3 first principal components

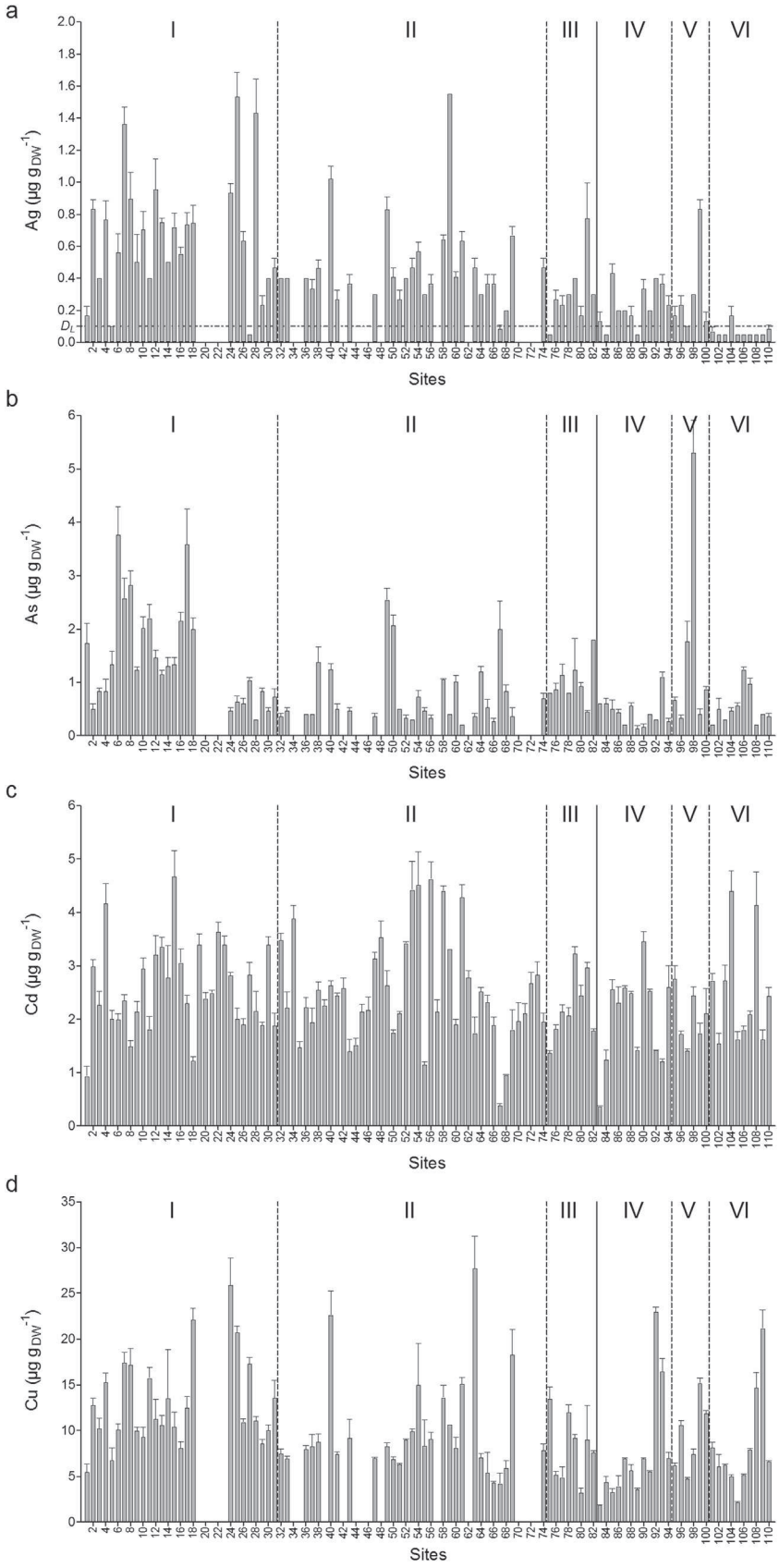

Fig. 2. a) Ag, b) As, c) Cd, d) Cu, e) Hg, f) Ni and g) Pb concentrations (mean ± SD, in µg g_{DW}^{-1}) measured in the blades of *Posidonia oceanica* adult leaves sampled between April and July of years 2003–2008 in 110 sites (numbers 1–110) located along the coasts of 13 Mediterranean countries, and Trace Element Pollution Index (TEPI) values (no unit) calculated from mean normalized TE concentrations. The Mediterranean was subdivided into 6 sub-areas (sub-areas I–VI, separated by dotted vertical lines), according to site location along its north-to-south and west-to-east axes. Sub-area I: European continental coasts; sub-area II: European insular coasts; sub-area III: North African coasts of the western Mediterranean; sub-area IV: western coasts of the eastern Mediterranean; sub-area V: Adriatic coasts; sub-area VI: coasts of the Aegean-Levantine basin. The full vertical line separates sub-areas of the western and the eastern Mediterranean, respectively. For clarity purpose, one in two site number is reported on graphs. Number of replicates $n = 3–5$, except for Hg in sites 2, 54, 56 ($n = 1$) and 4 ($n = 2$) and for Ag, As, Cd, Cu, Ni and Pb in site 59 ($n = 2$). The detection limit (D_L) of Ag analysis is reported on the Ag graph (dotted horizontal line).

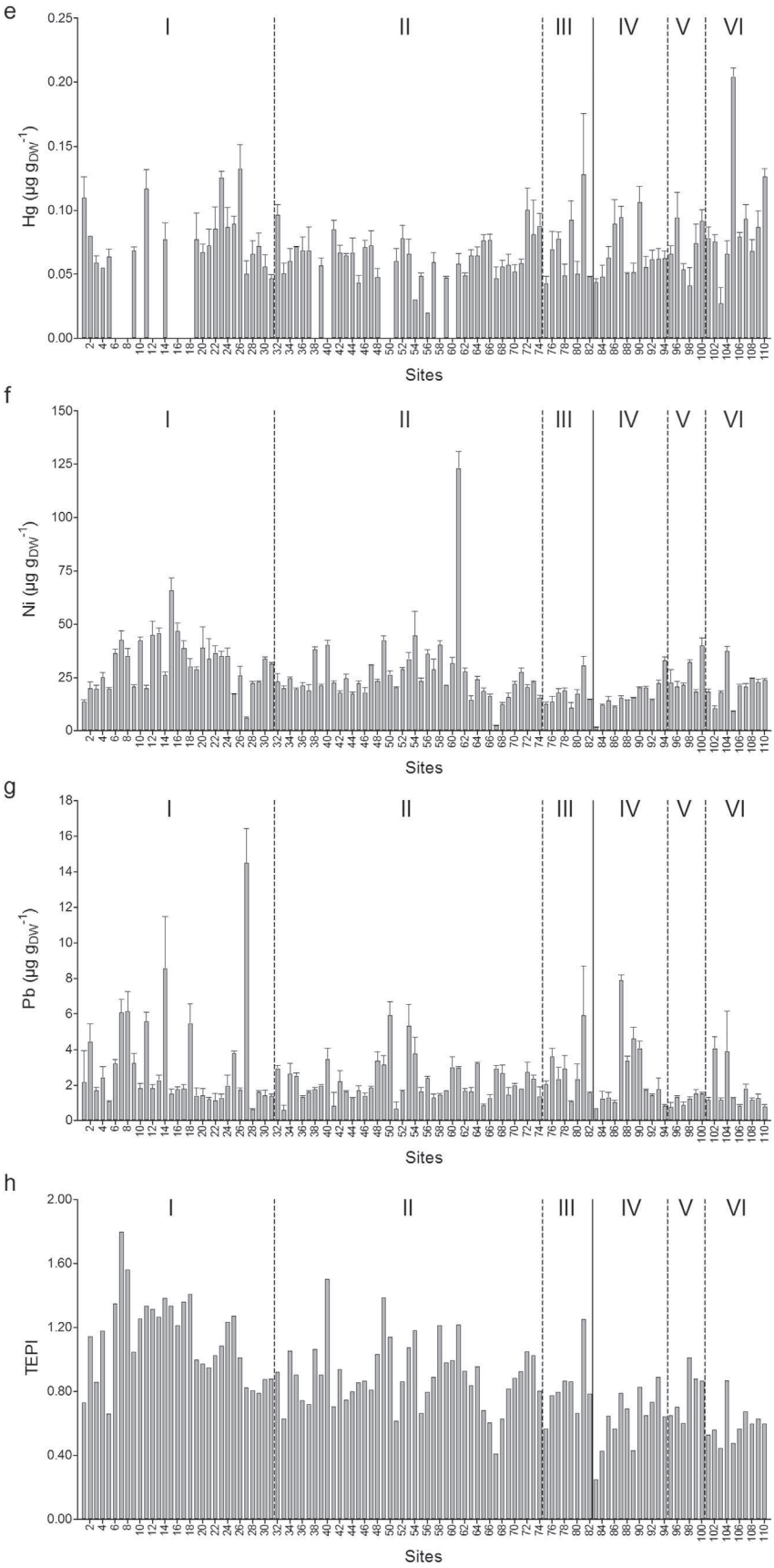

Fig. 2. (*continued*).

Table 1
Trace element (TE) concentrations (mean ± SD, in μg g_{DW}^{-1}) measured in the blades of *Posidonia oceanica* adult leaves sampled between April and July of years 2003–2008 in 110 sites located along the coasts of 13 Mediterranean countries, and Trace Element Pollution Index (TEPI) values (mean ± SD, no unit) calculated from mean normalized TE concentrations. The Mediterranean was subdivided into 6 sub-areas according to site location along its north-to-south and west-to-east axes. Sub-area I: European continental coasts; sub-area II: European insular coasts; sub-area III: North African coasts of the western Mediterranean; sub-area IV: western coasts of the eastern Mediterranean; sub-area V: Adriatic coasts; sub-area VI: coasts of the Aegean-Levantine basin. The number of sites sampled in each sub-area is given between brackets. Letters represent significant ($p < 0.05$) differences between sub-areas.

	Sub-area I (31)		Sub-area II (43)		Sub-area III (8)		Sub-area IV (12)		Sub-area V (6)		Sub-area VI (10)	
Ag	a	0.667 ± 0.378	ab	0.472 ± 0.279	abc	0.311 ± 0.214	bc	0.231 ± 0.128	abc	0.294 ± 0.274	c	0.067 ± 0.037
As	a	1.457 ± 0.945	b	0.752 ± 0.597	ab	1.001 ± 0.401	b	0.439 ± 0.267	ab	1.556 ± 1.906	b	0.520 ± 0.334
Cd		2.57 ± 0.84		2.51 ± 0.99		2.22 ± 0.62		2.01 ± 0.87		2.03 ± 0.50		2.51 ± 1.03
Cu	a	12.94 ± 4.85	ab	9.87 ± 5.34	ab	8.05 ± 3.56	b	7.36 ± 6.15	ab	9.32 ± 3.91	ab	8.31 ± 5.55
Hg		0.0789 ± 0.0242		0.0629 ± 0.0165		0.0697 ± 0.0292		0.0657 ± 0.0201		0.0701 ± 0.0209		0.0904 ± 0.0469
Ni		31.0 ± 12.1		26.6 ± 17.3		17.1 ± 6.2		16.2 ± 7.5		25.9 ± 8.4		20.7 ± 7.9
Pb		3.05 ± 2.84		2.19 ± 1.11		2.72 ± 1.51		2.50 ± 2.14		1.21 ± 0.31		1.74 ± 1.21
TEPI	a	1.127 ± 0.263	b	0.902 ± 0.214	ab	0.822 ± 0.202	b	0.630 ± 0.185	ab	0.786 ± 0.159	b	0.595 ± 0.119

(PCs; eigenvalues higher than 1) resulting from the PCA. Ag concentrations and TEPI values were the dominating features in the 1st PC (PC1) that explained 36.5% of the total variance of the data set. Cd and Hg concentrations showed the highest weights in the 2nd and 3rd PCs (PC2 and PC3) that explained 16.3% and 13.1% of the total variance, respectively (Table 4). The area defined by the dotted line on the 3D scores plot of samples in the space defined by the first 3 PCs (Fig. 4) contained the 15 sites the most highly contaminated by Ag, Cd or Hg, or showing the highest TEPI values (sites 19 and 73 excluded). Within this area were also found Cap Roux (16; France), very highly contaminated by Ni and As, Olbia (63; Sardinia, Italy), the most contaminated by Cu, Porto Ercole (27; Italy), highly contaminated by Cu and the most contaminated by Pb, Ajaccio Nord (50; Corsica, France), highly contaminated by As and very highly contaminated by Pb, and Marsaxlokk Bay (92; Malta) and Larnaca (109; Cyprus), very highly contaminated by Cu. The second area on the 3D scores plot defined by the full line contained 7 of the 15 sites with the lowest TEPI values, among them the cleanest Oristano (67; Sardinia, Italy), Monastir and Kerkena (83 and 84; Tunisia) sites. Urla (105, Turkey) was particular, as it showed the highest reported Hg level, contrasting with its very low TEPI value. Brbinjscica (98; Croatia), with the highest As concentration, a moderate Ag level, one of the lowest Hg concentrations, but a high TEPI value, had a particular position on the 3D scores plot.

The dendrogram (Fig. 5) resulting from the CA of the data set with TE concentrations and TEPI values showed 4 clusters at a linkage distance of 6. Results of multiple comparison tests of means between TE concentrations and TEPI values averaged by cluster are reported in Table 5. Specificities of each cluster could further be highlighted by sorting sampling sites on graphs as they appeared on the dendrogram, as illustrated for TEPI values in Fig. 6 (resulting graphs for the 7 TEs in Annex E). The extreme left cluster 1 (22 sites) grouped sites contaminated by Cd and some sites either highly contaminated by Ni or little impacted by As contamination; their corresponding TEPI values ranged from MCL to HCL. The central left cluster 2 (24 sites) grouped sites contaminated by Ag, As and/or Pb; their corresponding TEPI values ranged from HCL to VHCL. Conversely, the extreme right cluster 4 (40 sites) grouped sites little contaminated by TEs on the whole; their corresponding TEPI values ranged from VLCL to LCL. The last central right cluster 3 (24 sites) grouped sites moderately contaminated by TEs on the whole; their corresponding TEPI values ranged from LCL to MCL. The synthesis water quality map of the present study, overlaying TEPI values and clustering results (Annex C), is given in Fig. 3.

Highly significant ($p < 0.01$) positive correlations were found between Ag and Cd, Pb, Ni and Cu (weak to modest correlations), and between Ni and Cu and Cd (modest correlations). Highly significant ($p < 0.01$) positive correlations were further found between TEPI and all TEs except Hg (weak to strong correlations). Significant ($p < 0.05$) positive correlations were also found between Pb and As and Cu (weak; Fowler and Cohen, 1995; Table 6).

4. Discussion

4.1. An operational monitoring tool for a composite problem

The EU WFD (EC, 2000) and its Common Implementation Strategy for transitional and coastal waters (EC, 2003) are meant to promote the development of operational classification systems for sustainable coastal management. The holistic approach developed in the present study successfully led to the elaboration of such a classification system. In particular, the GIS mapping of Trace Element Pollution Index (TEPI) values, symbolized and colour-coded according to their contamination cluster and corresponding water quality scale level, resulted in a synthesis map that accurately outlined the chemical contamination severity along

Table 2
Coastal water quality scale (class-limits in μg g_{DW}^{-1}) derived from the quantile method, built from trace element (TE) concentrations measured in the blades of *Posidonia oceanica* adult leaves sampled between April and July of years 2003–2008 in 110 sites located along the coasts of 13 Mediterranean countries. The water quality scale is also given for the Trace Element Pollution Index (TEPI, no unit) calculated from mean normalized TE concentrations. The numbers between brackets represent, for each TE and for TEPI, the number of sites in each of the water quality 5 classes, with contamination levels (CL) ranging from very low (left) to very high (right).

	Very low CL	Low CL	Moderate CL	High CL	Very high CL
Ag	<0.091 (14)	0.091–0.281 (20)	0.281–0.439 (25)	0.439–0.892 (24)	>0.892 (8)
As	<0.299 (8)	0.299–0.499 (26)	0.499–0.923 (24)	0.923–2.123 (25)	>2.123 (8)
Cd	<1.42 (12)	1.42–2.07 (28)	2.07–2.57 (29)	2.57–3.65 (31)	>3.65 (10)
Cu	<4.71 (9)	4.71–7.53 (26)	7.53–10.24 (23)	10.24–17.72 (25)	>17.72 (8)
Hg	<0.0455 (7)	0.0455–0.0611 (28)	0.0611–0.0727 (25)	0.0727–0.1035 (26)	>0.1035 (8)
Ni	<13.3 (10)	13.3–20.2 (31)	20.2–25.8 (29)	25.8–42.3 (31)	>42.3 (9)
Pb	<1.03 (11)	1.03–1.54 (31)	1.54–2.19 (27)	2.19–4.84 (31)	>4.84 (10)
TEPI	<0.574 (11)	0.574–0.791 (29)	0.791–0.943 (30)	0.943–1.273 (28)	>1.273 (12)

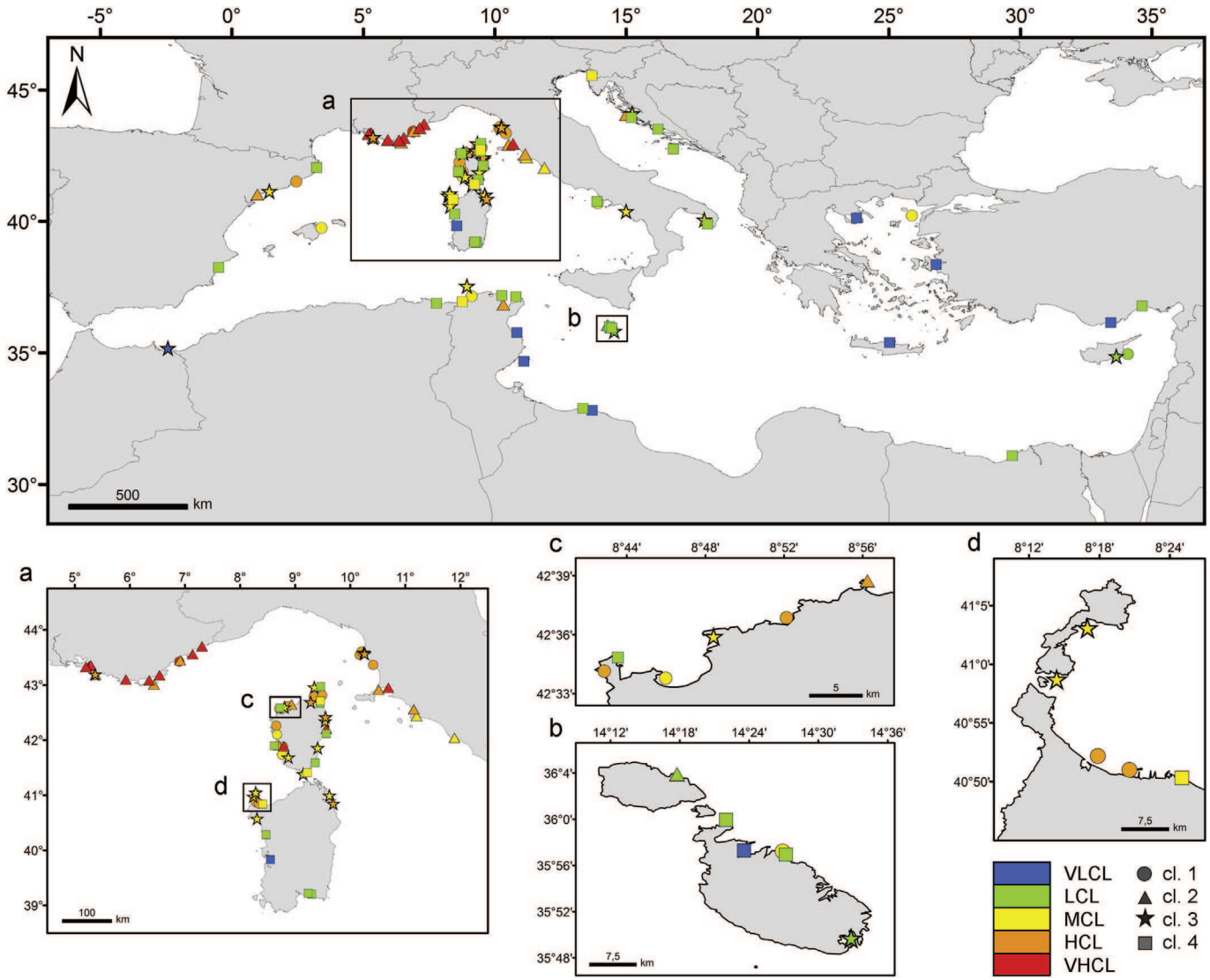

Fig. 3. Map of the global contamination by 7 trace elements in 110 sites located along the coasts of 13 Mediterranean countries, expressed as Trace Element Pollution Index (TEPI) values. TEPI values were calculated from mean normalized Ag, As, Cd, Cu, Hg, Ni and Pb concentrations measured in the blades of *Posidonia oceanica* adult leaves sampled between April and July of years 2003–2008. For clarity purpose, country names were not reported on the map (see Fig. 1). Site global contamination levels were GIS mapped according to a 5-level coastal water quality scale proposed using the quantile method, with contamination levels ranging from very low (VLCL, in blue) to very high (VHCL, in red; see Table 2). Sites were further clustered according to their contamination similarities (see Fig. 5 and Table 5) and each of the 4 resulting clusters (cl. 1–4) was symbolized by a geometric form. For clarity (site overlapping) and illustrative (different spatial scales) purposes, zooms were performed firstly on the northwestern Mediterranean area (zoomed area a; France and Italy) and on Malta (zoomed area b), and secondarily on the northwestern part of Corsica (zoomed area c) and Sardinia (zoomed area d). (For interpretation of the references to color in this figure legend, the reader is referred to the web version of this article.)

Mediterranean coasts (Fig. 3; Annex C). Overall, the TE contamination of the western Mediterranean displayed an evident north-to-south gradient, from the French and north-Italian continental coasts down through the insular Corsican and Sardinian coasts to the North African littoral. A second west-to-east gradient was observed between the 2 basins, the eastern Mediterranean being globally little to very little contaminated by TEs, except for a few sites proportionally more abundant in the northern Adriatic (Table 1; Figs 2h,3; Annexes B,C). These general trends have however to be considered with some reserve since part of the western Mediterranean, mainly the French and Italian coasts, was over represented compared to the rest of the Mediterranean.

TEPI values and TE levels (except Hg) were significantly ($p < 0.05$; Table 6) weakly to strongly-correlated with one another. Thus, Cd, As, Pb, Cu as well as Ni and Ag, in particular, all significantly contributed, with different degrees of severity, to the global contamination by TEs recorded along Mediterranean coasts. La Vesse (7; France), with the highest TEPI value (1.799), was an appropriate example of such composite problem as this site displayed high to very high Ag, As, Cu, Ni and Pb levels (Figs. 2,3; Annexes A,C). Since all TEs except Hg contributed to the global chemical contamination recorded along Mediterranean coasts, the efficient monitoring of this composite environmental threat clearly requires a multi-element approach to the problem (Luy et al., 2012; Richir and Gobert, 2014).

4.2. Ag

Ag found in the aquatic environment mainly originates in effluents from sewage treatment plants (Rozan and Hunter, 2001); Ag can therefore be used as a tracer of wastewater discharges in

Table 3
Trace Element Spatial Variation Index (TESVI) values calculated from mean Ag, As, Cd, Cu, Hg, Ni or Pb concentrations measured in the blades of *Posidonia oceanica* adult leaves sampled between April and July of years 2003–2008 in 110 sites located along the coasts of 13 Mediterranean countries. The number of sites (n = 91–110) analysed for each trace element (TE) is given between brackets. For each TE, x_{max}/x_{min} is the ratio between the maximum (x_{max}) and minimum (x_{min}) mean concentrations recorded among the n sites, and $\sum(x_{max}/x_i)/n$ (mean ± SD) is the mean ratio between the maximum mean concentration (x_{max}) and each of the n site mean concentrations (x_i). TESVI = $[(x_{max}/x_{min})/(\sum(x_{max}/x_i)/n)]$ * SD. The higher the TESVI value for a given TE, the more its levels globally varied throughout the whole Mediterranean.

		x_{max}/x_{min}	$\sum(x_{max}/x_i)/n$ ± SD	TESVI
Ag	(91)	31.0	8.3 ± 9.3	34.9
As	(91)	39.8	9.8 ± 7.3	29.4
Cd	(110)	12.7	2.3 ± 1.6	8.7
Cu	(91)	14.8	3.7 ± 2.3	9.2
Hg	(94)	10.2	3.2 ± 1.2	3.9
Ni	(110)	75.3	6.8 ± 8.4	92.7
Pb	(110)	24.2	8.7 ± 4.8	13.3

coastal waters (Muñoz-Barbosa et al., 2000; Chiffoleau et al., 2005). Ag VHCL in Ile Rousse (59, Corsica; Fig. 2a; Annexes A,C), also reported in previous studies (Lopez y Royo et al., 2009; Luy et al., 2012), thus could be attributed to the location of the sampling sites in the proximity of an urban sewage collector (Pergent et al., 2008). Ag showed, after Ni, the highest spatial variability of its environmental levels along coasts of the whole Mediterranean (TESVI value of 34.9; Table 3; Annex D) and displayed the most obvious north-to-south and west-to-east gradient decreases in concentrations (Table 1; Fig. 2a; Annexes B,C). Large scale biomonitoring surveys along the coasts of France and Baja California have demonstrated that sites affected by Ag contamination could be found relatively far (up to nearly 300 km away) from potential continental Ag sources, indicating the significant availability of Ag in saline water and its transport far from points of discharge (Muñoz-Barbosa et al., 2000; Chiffoleau et al., 2005). Continental sources of Ag can thus extensively affect large coastal areas (Chiffoleau et al., 2005), as shown in the present study through the diffuse Ag contamination along French and north Italian continental coasts and down to the insular Corsican littoral. Chiffoleau et al. (2005), who biomonitored the contamination by Ag with mussels and oysters along French coasts, however reported that the least contaminated areas in France were the Mediterranean coasts and northern Brittany. It is therefore appropriate to consider the Ag contamination reported in this study as of relatively limited importance.

Table 4
Factor loadings for the 3 first principal components (PC1, PC2, PC3) resulting from the principal component analysis of trace element concentrations measured in the blades of *Posidonia oceanica* adult leaves sampled between April and July of years 2003–2008 in 110 sites located along the coasts of 13 Mediterranean countries, and Trace Element Pollution Index (TEPI) values calculated from mean normalized TE concentrations. Factor loadings equal or greater than 0.700 in absolute terms are in bold.

	PC1	PC2	PC3
Ag	**−0.773**	−0.054	−0.077
As	−0.396	−0.547	0.505
Cd	−0.493	**0.715**	−0.069
Cu	−0.629	−0.196	−0.193
Hg	0.002	−0.109	**−0.809**
Ni	−0.694	0.472	0.178
Pb	−0.364	−0.438	−0.246
TEPI	**−0.955**	−0.146	−0.021

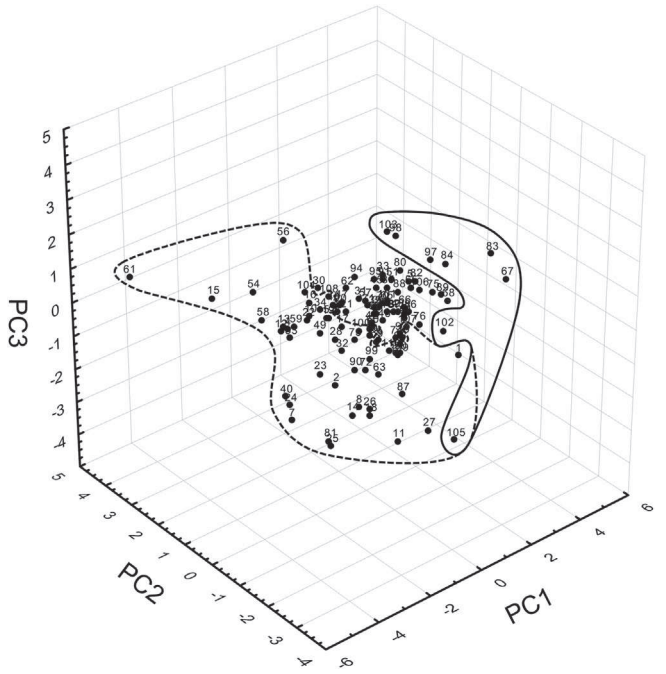

Fig. 4. Three-dimensional (3D) scores plot after principal component analysis of trace element (TE) concentrations measured in the blades of *Posidonia oceanica* adult leaves sampled between April and July of years 2003–2008 in 110 sites (numbers 1–110) located along the coasts of 13 Mediterranean countries, and Trace Element Pollution Index (TEPI) values calculated from mean normalized TE concentrations. Out of the 110 sampling sites, the 15 the most highly contaminated by Ag, Cd or Hg, or showing the highest TEPI values (sites 19 and 73 excluded) are contained on the 3D scores plot inside the area defined by the dotted line, as well as sites more specifically contaminated either by As, Cu, Ni and/or Pb. The second area on the 3D scores plot defined by the full line contains 7 of the 15 sites with the lowest TEPI values (site 98 excluded).

4.3. Cu, Ni and Cd

Although Cu, Ni and Cd occur naturally in trace concentrations in all ecosystems, mining, smelting activities and spill from abandoned mines have resulted in severe environmental contaminations by these metals (Garceau et al., 2010). They were therefore the contaminants of greatest concern in several areas such as major Canadian mining and smelting places in Sudbury (Ontario; Keller et al., 1992) and Rouyn-Noranda (Québec; Couillard et al., 1993). Likewise, correlations between Ni and Cu and Ni and Cd suggested common sources of contamination in the Mediterranean for these metals. Thus, VHCL in Cd and particularly in Ni reported for Canari (61; Corsica, France; Figs. 2c,f; Annexes A,C) resulted from the former asbestos mine of Canari, which discharged 11 million tons of rubble into the sea between 1948 and 1965 (Bernier et al., 1997). Other major anthropogenic sources of Cd in the environment include rock phosphate fertilizer and municipal and industrial refuse and sewage sludge (Järup and Åkesson, 2009; Pan et al., 2010). Mataro (4; Spain) has major industrial activities, and the visual assessment of human pressures highlighted the large scale agricultural (40%) and urban (44%) land use in this area (Lopez y Royo et al., 2009; Sánchez-Avila et al., 2009). The Cd VHCL in Mataro (Fig. 2c; Annexes A,C) was thus probably linked to the high urban sewage and agricultural inputs in its coastal environment (Lopez y Royo et al., 2009).

Cu, Pb and particularly Ni are important constituents of fuel oil. Their concentrations in salt marsh soils of Galicia (Northwestern Spain) following the 2002 Prestige oil spill were correlated with one another and with the total petroleum hydrocarbon content of the contaminated soils (Andrade et al., 2004). The Mediterranean is

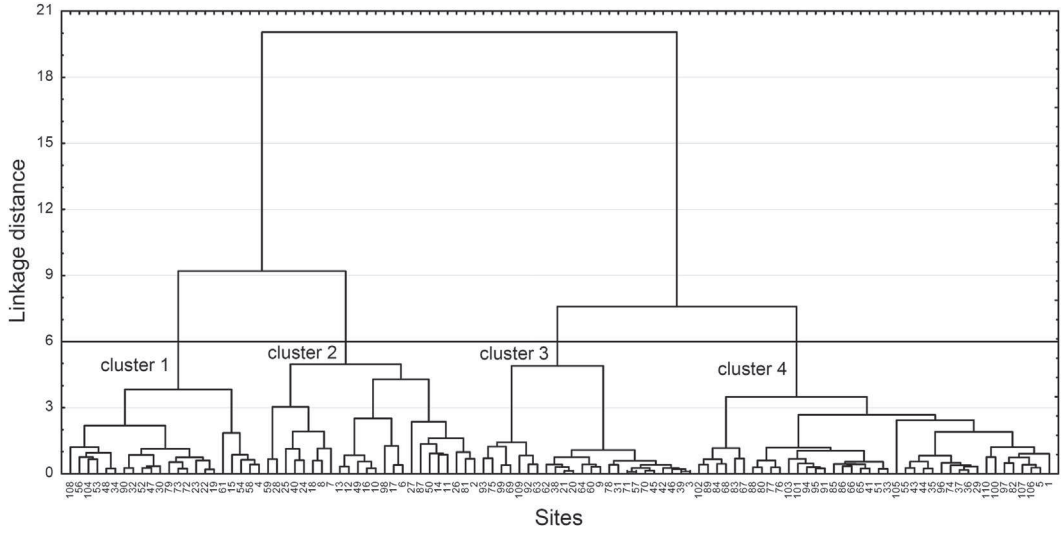

Fig. 5. Dendrographic classification after cluster analysis (Euclidean distance as measure of similarity) of Ag, As, Cd, Cu, Hg, Ni and Pb concentrations measured in the blades of *Posidonia oceanica* adult leaves sampled between April and July of years 2003–2008 in 110 sites (numbers 1–110) located along the coasts of 13 Mediterranean countries, and Trace Element Pollution Index (TEPI) values calculated from mean normalized TE concentrations. The dendrogram shows 4 clusters at a linkage distance of 6 (thick horizontal line).

Table 5
Trace element (TE) concentrations (mean ± SD, in $\mu g\ g_{DW}^{-1}$) measured in the blades of *Posidonia oceanica* adult leaves sampled between April and July of years 2003-2008 in 110 sites located along the coasts of 13 Mediterranean countries, and Trace Element Pollution Index (TEPI) values (mean ± SD, no unit) calculated from mean normalized TE concentrations, averaged by cluster observed at a linkage distance of 6 on the dendrogram resulting from the cluster analysis (Euclidean distance as measure of similarity) of TE concentrations and TEPI values. The number of sites in each cluster is given between brackets. Letters represent significant ($p < 0.05$) differences between clusters.

	Cluster 1 ($n = 22$)		Cluster 2 ($n = 24$)		Cluster 3 ($n = 24$)		Cluster 4 ($n = 40$)	
Ag	a	0.441 ± 0.198	a	0.777 ± 0.398	a	0.405 ± 0.205	b	0.205 ± 0.125
As	a	0.559 ± 0.386	b	1.698 ± 1.289	ab	0.780 ± 0.368	a	0.722 ± 0.473
Cd	a	3.78 ± 0.60	b	2.48 ± 0.59	c	2.05 ± 0.41	c	1.88 ± 0.60
Cu	a	10.50 ± 3.41	ab	13.24 ± 5.42	b	14.63 ± 6.12	c	6.16 ± 2.17
Hg		0.0721 ± 0.0254		0.0841 ± 0.0305		0.0605 ± 0.0109		0.0718 ± 0.0288
Ni	a	35.0 ± 22.6	ab	31.1 ± 11.1	ab	23.5 ± 7.3	b	18.0 ± 6.8
Pb	ab	2.40 ± 1.15	a	4.20 ± 3.12	bc	1.88 ± 0.62	c	1.66 ± 0.96
TEPI	abc	0.996 ± 0.174	b	1.234 ± 0.242	c	0.881 ± 0.113	d	0.646 ± 0.134

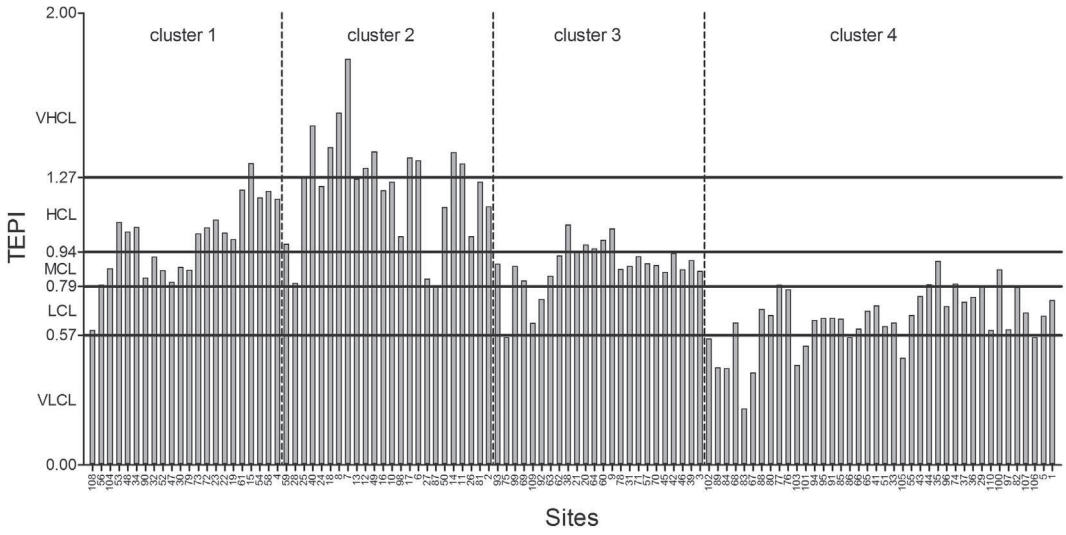

Fig. 6. Trace Element Pollution Index (TEPI) values (no unit) calculated from mean normalized Ag, As, Cd, Cu, Hg, Ni and Pb concentrations measured in the blades of *Posidonia oceanica* adult leaves sampled between April and July of years 2003–2008 in 110 sites (numbers 1–110) located along the coasts of 13 Mediterranean countries. Sampling sites are sorted on the graph according to the dendrographic classification after cluster analysis (Euclidean distance as measure of similarity) of trace element concentrations and TEPI values. Dotted vertical lines separate the 4 clusters shown on the dendrogram at a linkage distance of 6 (see Fig. 5). TEPI class-limit values (see Table 2) separating sites with global contamination levels considered either as very low (VLCL), low (LCL), medium (MCL), high (HCL) or very high (VHCL) are reported on the graph (full horizontal lines).

Table 6
Correlation matrix of parametric Pearson's correlation coefficients and non-parametric Spearman's rank correlation coefficients between trace element concentrations measured in the blades of *Posidonia oceanica* adult leaves sampled between April and July of years 2003–2008 in 110 sites located along the coasts of 13 Mediterranean countries, and Trace Element Pollution Index (TEPI) values calculated from mean normalized TE concentrations. Correlations significant at $p < 0.05$ are in bold; correlations significant at $p < 0.01$ are in bold underlined.

	Ag	As	Cd	Cu	Hg	Ni	Pb	TEPI
Ag	1.000							
As	0.204	1.000						
Cd	**0.291**	−0.168	1.000					
Cu	**0.549**	0.096	0.084	1.000				
Hg	0.008	−0.074	−0.043	−0.047	1.000			
Ni	**0.464**	0.178	**0.625**	**0.425**	0.006	1.000		
Pb	**0.294**	**0.252**	0.110	**0.261**	−0.014	0.126	1.000	
TEPI	**0.777**	**0.512**	**0.383**	**0.539**	0.132	**0.686**	**0.518**	1.000

a major loading and discharge center for crude oil (UNEP/MAP, 2012) and an important traffic zone for oil tankers (Jordi et al., 2006). In addition, a large number of oil-related sites (pipeline terminals, refineries, offshore platforms, etc.) are concentrated along the coastal zone, which together make the Mediterranean a particularly vulnerable area (Jordi et al., 2006). The abundance of Ni as a normal constituent of crude oils (Andrade et al., 2004), the high overall spatial variability of its levels along Mediterranean coasts (highest TESVI value of 92.7; Table 3; Annex D) and the relatively good cartographic concordance of Ni contamination and illicit oil spill density mapping (Annex C; UNEP/MAP, 2012), mainly in the eastern Mediterranean, are several indicators in favour of contamination due, at least in part, to hydrocarbons. Finally, the use of antifouling paints with Cu is common in harbour sheltering leisure boats subject to the anti-TBT legislation (Roméo et al., 2003; Obhođaš et al., 2006). The Cu VHCL in Olbia (63; Sardinia, Italy; Fig. 2d; Annexes A,C) could be linked to the intensive nautical tourism activity in the Gulf of Aranci (Augier et al., 1993). And on the slipways of Marsaxlokk (92; Malta), where boats are repaired and repainted, generated paint fragments and dusts are an additional direct source of Cu contamination in that bay (Huntingford and Turner, 2011).

4.4. Hg

In contrast to the other TEs, Hg contamination primarily affected the coasts of the Aegean–Levantine basin in the eastern Mediterranean, and secondarily the European continental coasts of the western Mediterranean (Table 1; Fig. 2e; Annexes B,C). This observation coincides with the spatial distribution of current major anthropogenic Hg emission sources, mainly located in Mediterranean countries of the Levantine basin (UNEP/MAP/MED POL, 2011a). Hg, contrary to the other TEs, did not significantly contribute to the global contamination by TEs recorded along Mediterranean coasts (Table 6). Hg further displayed the lowest overall spatial variability of its environmental levels (TESVI value of 3.9; Table 3; Annex D). This relative lack of spatial variability could reflect the general decrease in Hg production and emission in the Mediterranean area (UNEP/MAP/MED POL, 2011a), associated with an overall decreasing trend in Hg concentrations in several bioindicator species (UNEP/MAP/MED POL, 2011a; Copat et al., 2012; Borrell et al., 2014). Among TEs considered toxic and of environmental concern, Hg appears to be the most highly poisonous to marine life (Davies, 1978; Shahidul Islam and Tanaka, 2004). Consequently, even small variations in coastal Hg levels must be regarded as threatening. Local Hg contaminations are either of natural origin, *i.e.* the presence of cinnabar deposits (HgS) and volcanoes, or of anthropogenic origin in the vicinity of harbours, industrial facilities or mining activities (Cossa and Coquery, 2005). The Hg VHCL in Urla (105; Turkey; Fig. 2e; Annexes A,C) was thus related to the major cinnabar mining activities undertaken in that area (Gemici, 2008). Although the mines were abandoned gradually up until the early 1990s, they continue to deliver considerable quantities of Hg to the river system and many km downstream, especially in Urla (near the abandoned Kalecik mine; Gemici and Oyman, 2003).

4.5. As and Pb

Similarly to Hg, the lack of any important correlation between Pb and particularly As and any other TEs suggested more specific sources of contamination for these elements. However, conversely to Hg, both Pb and As modestly contributed to the global contamination by TEs (Table 6). As is an ubiquitous element in the environment. Most environmental As problems are the result of its mobilisation under natural conditions (Smedley and Kinniburgh, 2002). Previous results obtained on As in mussels from various districts in the Adriatic suggested the influence of hydrological, oceanographic and meteorological conditions of the Adriatic Sea in modulating the natural biogeochemistry and accumulation of this element in marine life (Fattorini et al., 2008). It is however unlikely that the As VHCL at Brbinjscica (98; Dugi Otok island, Croatia; Fig. 2b; Annexes A,C), away from any major source of As contamination (Salivas-Decaux et al., 2009), arose solely from this general environmental influence. The island of Dugi Otok is predominantly composed of karstified carbonate rocks. The dominating substrate is limestone and dolomite on which *terra rossa*, red earth, has formed (Terzić et al., 2007; Bašic, 2013). Limestone and dolomitic rocks can contain high concentrations of As (Wunsch et al., 2013, 2014), and *terra rossa* soil has naturally higher As contents than other types of soils (Lovrenčić Mikelić et al., 2013). The majority of coastal karst aquifers are further anchialine environments (Cuculić et al., 2011). Enhanced concentrations of total and dissolved Cd, Pb, Cu and Zn were reported in 2 Croatian anchialine caves (Cuculić et al., 2011), and high As levels in surface sediments were systematically reported in 6 anchialine caves along the Croatian Adriatic coast (Cukrov et al., 2009). Similarly, potentially As-enriched underground water from Dugi Otok karstified aquifers could have enhanced As concentrations in brackish, saline waters and coastal sediments in the Brbinjscica area, resulting in the As VHCL reported for this site. In addition to the natural mobilisation of As in the environment, man has had a strong impact on contamination by this element (Smedley and Kinniburgh, 2002). High As concentrations compared to the estuarine water baseline were reported in several European estuaries affected by industrial or mining effluents (*e.g.* Tamar, Scheldt and Loire estuaries; Smedley and Kinniburgh, 2002). Similarly, the As VHCL observed along Marseille littoral (6–8; France), as well as its Pb VHCL (7–8; Figs. 2b,g; Annexes A,C), also reflected the highly industrialised history of this area (Lassalle, 2007).

Regarding Pb, the biogeochemical cycle of that TE has been affected by man to a great degree (Komárek et al., 2008). Several surveys reported Pb levels in Portmán sediments and biota, Spain, one to two orders of magnitude higher than concentrations found in other areas (César et al., 2004; Benedicto et al., 2008; Martínez-Gómez et al., 2012); this contamination was explained by past mining activities and inputs from various industrial activities from Escombreras Valley (Cartagena; UNEP/MAP/MED POL, 2011b). Similarly, Pb VHCL at Porto Ercole (27; Italy; Fig. 2g; Annexes A,C) seemed to be related to past human activities. This sampling site was indeed located in the southern side of the previously highly industrialized Orbetello lagoon, facing an old Fe–Mn mineral extraction site active from 1873 until 1958 whose metal enriched residual waste was discharged directly in the lagoon (Mester et al., 1998; Pepi et al., 2009; Romano and Ausili, 2012). Marine sediments and animals from Maltese coastal waters were found to be contaminated by hydrocarbons of fossil fuel origin, probably in the form of minute pelagic tar particulates, although fossil fuels of local origin such as those used in pleasure crafts may also have been a contributing factor (Sammut and Nickless, 1978 in Huntingford and Turner, 2011). Since Pb was reported to be strongly correlated to total petroleum hydrocarbon contamination (Andrade et al., 2004), the contamination of the Maltese coasts with hydrocarbons could explain in part the high to very high Pb levels reported in that area (Fig. 2g; Annexes A,C). However, no concomitant contamination by Ni or Cu was observed, suggesting that the source of Pb contamination could be different. In the case of Bahar ic-Caghaq (90), high trace element levels including Pb in sediments and biota were thus attributed to the immediate vicinity of the Maghtab landfill (Wilson, 2004).

5. Conclusion

Sustained monitoring programs are necessary to evidence the efficacy of regulatory controls on pollutant discharges to the environment and to define the relative health status of ecosystems. Within this perspective, the present study aimed to monitor for the first time the coastal contamination of the entire Mediterranean by Ag, As, Cd, Cu, Hg, Ni and Pb, using *P. oceanica* as bioindicator species. But sustainable coastal management also requires the development of appropriate contamination classification systems intended, among other purposes, for environmental managers and policy makers. The combined utilization of several complementary monitoring tools, *i.e.* water quality scale, pollution index (TEPI and TESVI) and spatial analysis (PCA, CA, correlation analysis and GIS mapping) successfully led to the development of an operational classification system of this kind. This classification system enabled us to globally assess TE contamination threats and to depict contamination gradients at the scale of the entire Mediterranean, while monitoring TE contamination impacts at more regional or local scales. In conclusion, such holistic approaches should be privileged to accurately monitor the TE contamination rate of coastal waters and to transfer relevant information on this composite problem to environmental managers and policy makers.

Acknowledgements

Funding was provided by the Territorial Collectivity of Corsica, the French Water Agency, the FRS-FNRS (FRFC 2.4.502.08) and the French Community of Belgium (ARC RACE 05/10-333). This study is part of the STARECAPMED project, and was supported by the collaboration of several laboratories from all around the Mediterranean: Dr Saïd Belbacha and Dr Rachid Semroud (Algeria); University of Zagreb, scientific project no. 119-0362975-1226, project coordinator Dr Tatjana Bakran-Petricioli (Croatia); Melina Marcou and Myroula Hadjichristoforou (Cyprus); Dr Stéphane Sartoretto, Ifremer Center of Toulon, Dr Pierre Lejeune, STARESO, and Berangère Casalta (France); Dr Georges Skoufas and Dr Eugenia Apostolaki, Institute of Oceanography, Hellenic Centre for Marine Research (Greece); Dr Cristina Buia and Dr Pier Panzalis (Italy); Dr Joseph Borg (Malta); Robert Turk, Borut Mavric and Lovrenc Lipej (Slovenia); Boris Weitzmann, Dr Yolanda Fernandez Torquemade, F. Javier Zapata Salgado, Elvira Alvarez Pérez, Dr Javier Romero, Izaskun Llagostera (Spain); Dr Habib Langar (Tunisia); Dr Baris Akçalı and Billür Celebi (Turkey). We also thank Steven Barillec, Nicolas Luy and Renzo Biondo for their help. This publication has the MARE publication number MARE280.

Appendix A. Supplementary data

Supplementary data related to this article can be found at http://dx.doi.org/10.1016/j.jenvman.2014.11.015.

References

Agardy, T., Alder, J., Dayton, P., Curran, S., Kitchingman, A., et al., 2005. Chapter 19: coastal systems. In: Hassan, R., Scholes, R., Ash, N. (Eds.), Ecosystems and Human Well-being: Current State and Trends, vol. 1. Island Press, Washington, DC, pp. 513–549.

Amiard, J.C., 2011. Les risques chimiques environementaux: méthodes d'évaluation et impacts sur les organismes. Tec & doc-Lavoisier, Paris, France.

Ancora, S., Bianchi, N., Butini, A., Buia, M.C., Gambi, M.C., et al., 2004. *Posidonia oceanica* as a biomonitor of trace elements in the Gulf of Naples: temporal trends by lepidochronology. Environ. Toxicol. Chem. 23 (5), 1093–1099.

Andrade, M.L., Covelo, E.F., Vega, F.A., Marcet, P., 2004. Effect of the Prestige oil spill on salt marsh soils on the coast of Galicia (Northwestern Spain). J. Environ. Qual. 33 (6), 2103–2120.

Augier, H., Harmand-Desforges, J.M., Ramonda, G., 1993. Pleasure harbours are responsible for the metallic contamination of *Posidonia oceanica* meadows. In: First International Conference on the Mediterranean Coastal Environment, Antalya, Turkey, pp. 127–141. MEDCOAST.

Bašic, F., 2013. The Soils of Croatia. Springer, Dordrecht Heidelberg, New York, London.

Benedicto, J., Martínez-Gómez, C., Guerrero, J., Jornet, J., Rodríguez, C., 2008. Metal contamination in Portmán Bay (Murcia, SE Spain) 15 years after the cessation of mining activities. Cienc. Mar. 34 (3), 389–398.

Bernier, P., Guidi, J.-B., Böttcher, M.E., 1997. Coastal progradation and very early diagenesis of ultramafic sands as a result of rubble discharge from asbestos excavations (northern Corsica, western Mediterranean). Mar. Geol. 144 (1–3), 163–175.

Bethoux, J.P., Courau, P., Nicolas, E., Ruizpino, D., 1990. Trace metal pollution in the Mediterranean Sea. Oceanol. Acta 13 (4), 481–488.

Blandin, P., 1986. Bioindicateurs et diagnostic des systémes écologiques. Bull. Ecol. 17, 211–307.

Borrell, A., Aguilar, A., Tornero, V., Drago, M., 2014. Concentrations of mercury in tissues of striped dolphins suggest decline of pollution in Mediterranean open waters. Chemosphere 107, 319–323.

Boudouresque, C.F., Bernard, G., Bonhomme, P., Charbonnel, E., Diviacco, G., et al., 2012. Protection and Conservation of *Posidonia oceanica* Meadows. RAMOGE and RAC/SPA Publisher, Tunis.

Burger, J., 2006. Bioindicators: a review of their use in the environmental literature 1970–2005. Environ. Bioindic. 1, 136–144.

Callender, E., 2003. Heavy metals in the environment - historical trends. In: Holland, H.D., Turekian, K.K. (Eds.), Treatise on Geochemistry, vol. 9. Elsevier, pp. 67–105.

Capiomont, A., Piazzi, L., Pergent, G., 2000. Seasonal variations of total mercury in foliar tissues of *Posidonia oceanica*. J. Mar. Biol. Assoc. U.K. 80 (6), 1119–1123.

César, A., Marín, L., Marín-Guirao, A., Vita, A., 2004. Amphipod and sea urchin test to assess the toxicity of Mediterranean sediments: the case of Portmán Bay. Cienc. Mar. 68 (S1), 205–213.

Chiffoleau, J.F., Auger, D., Roux, N., Rozuel, E., Santini, A., 2005. Distribution of silver in mussels and oysters along the French coasts: data from the national monitoring program. Mar. Pollut. Bull. 50 (12), 1719–1723.

Conti, M.E., Bocca, B., Iacobucci, M., Finoia, M.G., Mecozzi, M., et al., 2010. Baseline trace metals in seagrass, algae, and mollusks in a southern tyrrhenian ecosystem (Linosa Island, Sicily). Arch. Environ. Contam. Toxicol. 58 (1), 79–95.

Copat, C., Maggiore, R., Arena, G., Lanzafame, S., Fallico, R., et al., 2012. Evaluation of a temporal trend heavy metals contamination in *Posidonia oceanica* (L.) Delile, (1813) along the Western coastline of Sicily (Italy). J. Environ. Monit. 14 (1), 187–192.

Cossa, D., Coquery, M., 2005. The Mediterranean mercury anomaly, a geochemical or a biological issue. In: Saliot, A. (Ed.), The Mediterranean Sea, 5K. Springer, Berlin Heidelberg, pp. 177–208.

Couillard, Y., Campbell, P.G.C., Tessier, A., 1993. Response of metallothionein concentrations in a freshwater bivalve (*Anodonta grandis*) along an environmental cadmium gradient. Limnol. Oceanogr. 38 (2), 299–313.
Cozza, R., Iaquinta, A., Cozza, D., Ruffolo, L., 2013. Trace metals in *Posidonia oceanica* in a coastal area of the Ionian Sea (Calabria, Italy). Open J. Ecol. 3 (2), 102–108.
Cuculić, V., Cukrov, N., Željko, K., Mlakar, M., 2011. Distribution of trace metals in anchialine caves of Adriatic Sea, Croatia. Estuar. Coast. Shelf Sci. 95 (1), 253–263.
Cukrov, N., Kwokal, Ž., Cuculić, V., Omanović, D., Jalžić, D., 2009. Ecotoxic metal concentrations in sediment from Croatians anchialine caves. Anchialine ecosystems: Reflection and prospects, Palma de Mallorca, Spain. Poster presentation.
Davies, A.G., 1978. Pollution studies with marine plankton. Part II - Heavy metals. In: Frederick, S.R., Maurice, Y. (Eds.), Advances in Marine Biology, vol. 15. Academic Press, pp. 381–508.
Durrieu de Madron, X., Guieu, C., Sempéré, R., Conan, P., Cossa, D., et al., 2011. Marine ecosystems' responses to climatic and anthropogenic forcings in the Mediterranean. Prog. Oceanogr. 91 (2), 97–166.
EC, 2000. Directive 2000/60/EC of the European Parliament and the Council of 23 October 2000 establishing a framework for Community action in the field of water policy. Off. J. Eur. Commun. L 327/1, 22.12.2000.
EC, 2002. Recommendation of the European Parliament and of the Council of 30 May 2002 concerning the implementation of Integrated Coastal Zone Management in Europe (2002/413/EC). Off. J. Eur. Commun. L 148/24, 6.6.2002.
EC, 2003. Common implementation strategy for the water framework directive (2000/60/EC). Guidance document no 5. Transitional and coastal waters - typology, reference conditions and classification systems.
EC, 2008. Directive 2008/56/EC of the European Parliament and of the Council of 17 June 2008 establishing a framework for community action in the field of marine environmental policy (Marine Strategy Framework Directive). Off. J. Eur. Commun. L 164/19, 25.6.2008.
Fattorini, D., Notti, A., Di Mento, R., Cicero, A.M., Gabellini, M., et al., 2008. Seasonal, spatial and inter-annual variations of trace metals in mussels from the Adriatic sea: a regional gradient for arsenic and implications for monitoring the impact of off-shore activities. Chemosphere 72 (10), 1524–1533.
Foden, J., Brazier, D.P., 2007. Angiosperms (seagrass) within the EU water framework directive: a UK perspective. Mar. Pollut. Bull. 55 (1–6), 181–195.
Fowler, J., Cohen, L., 1995. Practical Statistics for Field Biology. John Wiley & Sons Ltd., Baffins Lane, Chichester West Sussex PO19 1UD, England.
Garceau, N., Pichaud, N., Couture, P., 2010. Inhibition of goldfish mitochondrial metabolism by *in vitro* exposure to Cd, Cu and Ni. Aquat. Toxicol. 98 (2), 107–112.
Gemici, Ü., 2008. Evaluation of the water quality related to the acid mine drainage of an abandoned mercury mine (Alaşehir, Turkey). Environ. Monit. Assess. 147 (1–3), 93–106.
Gemici, Ü., Oyman, T., 2003. The influence of the abandoned Kalecik Hg mine on water and stream sediments (Karaburun, İzmir, Turkey). Sci. Total Environ. 312 (1–3), 155–166.
Gobert, S., Cambridge, M.L., Velimirov, B., Pergent, G., Lepoint, G., et al., 2006. Biology of *Posidonia*. In: Larkum, A.W.D., Orth, R.J., Duarte, C.M. (Eds.), Seagrasses: Biology, Ecology and Conservation. Springer, Dordrecht, The Netherlands, pp. 387–408.
Huntingford, E.J., Turner, A., 2011. Trace metals in harbour and slipway sediments from the island of Malta, central Mediterranean. Mar. Pollut. Bull. 62 (7), 1557–1561.
Järup, L., Åkesson, A., 2009. Current status of cadmium as an environmental health problem. Toxicol. Appl. Pharmacol. 238 (3), 201–208.
Jordi, A., Ferrer, M.I., Vizoso, G., Orfila, A., Basterretxea, G., et al., 2006. Scientific management of Mediterranean coastal zone: a hybrid ocean forecasting system for oil spill and search and rescue operations. Mar. Pollut. Bull. 53 (5–7), 361–368.
Keller, W., Gunn, J.M., Yan, N.D., 1992. Evidence of biological recovery in acid-stressed lakes near Sudbury, Canada. Environ. Pollut. 78 (1–3), 79–85.
Komárek, M., Ettler, V., Chrastný, V., Mihaljevič, M., 2008. Lead isotopes in environmental sciences: a review. Environ. Int. 34 (4), 562–577.
Lafabrie, C., Pergent, G., Kantin, R., Pergent-Martini, C., Gonzalez, J.L., 2007a. Trace metals assessment in water, sediment, mussel and seagrass species - validation of the use of *Posidonia oceanica* as a metal biomonitor. Chemosphere 68 (11), 2033–2039.
Lafabrie, C., Pergent, G., Pergent-Martini, C., Capiomont, A., 2007b. *Posidonia oceanica*: a tracer of past mercury contamination. Environ. Pollut. 148 (2), 688–692.
Lafabrie, C., Pergent-Martini, C., Pergent, G., 2008. Metal contamination of *Posidonia oceanica* meadows along the Corsican coastline (Mediterranean). Environ. Pollut. 151, 262–268.
Lafabrie, C., Pergent, G., Pergent-Martini, C., 2009. Utilization of the seagrass *Posidonia oceanica* to evaluate the spatial dispersion of metal contamination. Sci. Total Environ. 407 (7), 2440–2446.
Lassalle, J.L., 2007. Présence de plomb et d'arsenic sur le littoral sud de Marseille: une étude de santé. Institut de Veille Sanitaire, France. Saint-Maurice.
Lewis, M.A., Devereux, R., 2009. Non-nutrient anthropogenic chemicals in seagrass ecosystems: fate and effects. Environ. Toxicol. Chem. 28 (3), 644–661.
Lopez y Royo, C., Pergent, G., Alcoverro, T., Buia, M.C., Casazza, G., et al., 2011. The seagrass *Posidonia oceanica* as indicator of coastal water quality: experimental intercalibration of classification systems. Ecol. Indic. 11 (2), 557–563.
Lopez y Royo, C., Silvestri, C., Salivas-Decaux, M., Pergent, G., Casazza, G., 2009. Application of an angiosperm-based classification system (BiPo) to Mediterranean coastal waters: using spatial analysis and data on metal contamination of plants in identifying sources of pressure. Hydrobiologia 633 (1), 169–179.
Lovrenčić Mikelić, I., Oreščanin, V., Barišić, D., 2013. Distribution and origin of major, minor, and trace elements in sediments and sedimentary rocks of the Kaštela Bay (Croatia) coastal area. J. Geochem. Explor. 128 (0), 1–13.
Luy, N., Gobert, S., Sartoretto, S., Biondo, R., Bouquegneau, J.M., et al., 2012. Chemical contamination along the Mediterranean French coast using *Posidonia oceanica* (L.) Delile above-ground tissues: a multiple trace element study. Ecol. Indic. 18 (1), 269–277.
Martínez, M.L., Intralawan, A., Vázquez, G., Pérez-Maqueo, O., Sutton, P., et al., 2007. The coasts of our world: ecological, economic and social importance. Ecol. Econ. 63 (2–3), 254–272.
Martínez-Gómez, C., Fernández, B., Benedicto, J., Valdés, J., Campillo, J.A., et al., 2012. Health status of red mullets from polluted areas of the Spanish Mediterranean coast, with special reference to Portmán (SE Spain). Mar. Environ. Res. 77, 50–59.
Mester, Z., Cremisini, C., Ghiara, E., Morabito, R., 1998. Comparison of two sequential extraction procedures for metal fractionation in sediment samples. Anal. Chim. Acta 359 (1–2), 133–142.
Montefalcone, M., 2009. Ecosystem health assessment using the Mediterranean seagrass *Posidonia oceanica*: a review. Ecol. Indic. 9 (4), 595–604.
Moreda-Pineiro, A., Marcos, A., Fisher, A., Hill, S.J., 2001. Evaluation of the effect of data pre-treatment procedures on classical pattern recognition and principal components analysis: a case study for the geographical classification of tea. J. Environ. Monit. 3 (4), 352–360.
Muñoz-Barbosa, A., Gutiérrez-Galindo, E.A., Flores-Muñoz, G., 2000. *Mytilus californianus* as an indicator of heavy metals on the northwest coast of Baja California, Mexico. Mar. Environ. Res. 49 (2), 123–144.
Nobre, A.M., 2011. Scientific approaches to address challenges in coastal management. Mar. Ecol. Prog. Ser. 434, 279–289.
Nordberg, G.F., Fowler, B.A., Nordberg, M., Friberg, L.T., 2007. Handbook on the Toxicology of Metals, third ed. Elsevier Inc.
Obhođaš, J., Kutle, A., Valković, V., 2006. Concentrations of some elements in the coastal sea sediments: bays with marinas. J. Radioanal. Nucl. Chem. 270 (1), 75–85.
Orth, R.J., Carruthers, T.J.B., Dennison, W.C., Duarte, C.M., Fourqurean, J.W., et al., 2006. A global crisis for seagrass ecosystems. Bioscience 56 (12), 987–996.
Pan, J., Plant, J., Voulvoulis, N., Oates, C., Ihlenfeld, C., 2010. Cadmium levels in Europe: implications for human health. Environ. Geochem. Health 32 (1), 1–12.
Pepi, M., Lobianco, A., Renzi, M., Perra, G., Bernardini, E., et al., 2009. Two naphthalene degrading bacteria belonging to the genera Paenibacillus and Pseudomonas isolated from a highly polluted lagoon perform different sensitivities to the organic and heavy metal contaminants. Extremophiles 13 (5), 839–848.
Pergent, G., Leonardini, R., Lopez y Royo, C., Mimault, B., Pergent-Martini, C., 2008. Mise en oeuvre d'un Réseau de Surveillance Posidonies le long du littoral de la Corse – Rapport de synthèse 2004-2008. Contrat office de l'Environnement de la Corse et GIS Posidonie centre de Corse. Corte.
Pergent, G., Bazairi, H., Bianchi, C.N., Boudouresque, C.F., Buia, M.C., et al., 2012. Mediterranean Seagrass Meadows: Resilience and Contribution to Climate Change Mitigation. A Short Summary. IUCN, Gland, Switzerland and Málaga, Spain.
Pergent-Martini, C., Leoni, V., Pasqualini, V., Ardizzone, G.D., Balestri, E., et al., 2005. Descriptors of *Posidonia oceanica* meadows: use and application. Ecol. Indic. 5 (3), 213–230.
Phillips, D.J.H., 1994. Macrophytes as biomonitors of trace metals. In: Kramer, K.J.M. (Ed.), Biomonitoring of Coastal Waters and Estuaries. CRC Press, Boca Raton, Florida, pp. 85–106.
Procaccini, G., Buia, M.-C., Gambi, M.-C., Perez, M., Pergent, G., et al., 2003. The seagrasses of the western Mediterranean. In: Green, E.P., Short, F.T. (Eds.), World Atlas of Seagrasses, pp. 48–58.
Rainbow, P.S., 2006. Biomonitoring of trace metals in estuarine and marine environments. Australas. J. Ecotoxicol. 12, 107–126.
Ralph, P.J., David, T., Kenneth, M., Stephanie, S., Macinnis-Ng, C.M.O., 2006. Human impacts on seagrasses: eutrophication, sedimentation, and contamination. In: Larkum, A.W.D., Orth, R.J., Duarte, C.M. (Eds.), Seagrasses: Biology, Ecology and Conservation. Springer, Dordrecht, The Netherlands, pp. 567–593.
Richir, J., Gobert, S., 2014. A reassessment of the use of *Posidonia oceanica* and *Mytilus galloprovincialis* to biomonitor the coastal pollution of trace elements: new tools and tips. Mar. Pollut. Bull. 89, 390–406.
Richir, J., Luy, N., Lepoint, G., Rozet, E., Alvera Azcarate, A., et al., 2013. Experimental *in situ* exposure of the seagrass *Posidonia oceanica* (L.) Delile to 15 trace elements. Aquat. Toxicol. 140–141, 157–173.
Romano, E., Ausili, A., 2012. Mercury contamination on Italian marine coastal areas due to industrial and mining activities. Workshop on Mercury management and decontamination, Almaden, Spain. Regional Activity Centre for Sustainable Consumption and Production (SCP/RAC). Oral presentation.
Roméo, M., Hoarau, P., Garello, G., Gnassia-Barelli, M., Girard, J.P., 2003. Mussel transplantation and biomarkers as useful tools for assessing water quality in the NW Mediterranean. Environ. Pollut. 122 (3), 369–378.
Rozan, T.F., Hunter, K.S., 2001. Effects of discharge on silver loading and transport in the Quinnipiac River, Connecticut. Sci. Total Environ. 279 (1–3), 195–205.

Salivas-Decaux, M., Alglave, C., Ferrat, T., Bakran-Petricioli, T., Turk, R., et al., 2009. Evaluation of trace-metal contamination in the northeastern Adriatic coastal waters using the seagrass *Posidonia oceanica*. Nat. Conserv. 22, 147–156.

Sammut, M., Nickless, G., 1978. Petroleum hydrocarbons in marine-sediments and animals from island of Malta. Environmental Pollution 16, 17–30.

Sánchez-Avila, J., Bonet, J., Velasco, G., Lacorte, S., 2009. Determination and occurrence of phthalates, alkylphenols, bisphenol A, PBDEs, PCBs and PAHs in an industrial sewage grid discharging to a Municipal Wastewater Treatment Plant. Sci. Total Environ. 407 (13), 4157–4167.

Sanchiz, C., Garcia-Carrascosa, A.M., Pastor, A., 2000. Heavy metal contents in soft-bottom marine macrophytes and sediments along the Mediterranean coast of Spain. Mar. Ecol. Public. della Stazion. Zool. Napoli 21 (1), 1–16.

Sardá, R., Avila, C., Mora, J., 2005. A methodological approach to be used in integrated coastal zone management processes: the case of the Catalan Coast (Catalonia, Spain). Estuar. Coast. Shelf Sci. 62 (3), 427–439.

Serrano, O., Mateo, M.A., Dueñas-Bohórquez, A., Renom, P., López-Sáez, J.A., et al., 2011. The *Posidonia oceanica* marine sedimentary record: a Holocene archive of heavy metal pollution. Sci. Total Environ. 409 (22), 4831–4840.

Shahidul Islam, M., Tanaka, M., 2004. Impacts of pollution on coastal and marine ecosystems including coastal and marine fisheries and approach for management: a review and synthesis. Mar. Pollut. Bull. 48 (7–8), 624–649.

Smedley, P.L., Kinniburgh, D.G., 2002. A review of the source, behaviour and distribution of arsenic in natural waters. Appl. Geochem. 17 (5), 517–568.

Terzić, J., Šumanovac, F., Buljan, R., 2007. An assessment of hydrogeological parameters on the karstic island of Dugi Otok, Croatia. J. Hydrol. 343 (1–2), 29–42.

UNEP/MAP, 1996. Etat du milieu marin et littoral de la region mediterranéenne. UNEP/MAP – Barcelona Convention. Athens.

UNEP/MAP, 2011. Convention for the Protection of the Marine Environment and the Coastal Region of the Mediterranean and its Protocols. UNEP/MAP – Barcelona Convention. Athens.

UNEP/MAP, 2012. State of the Mediterranean Marine and Coastal Environment. UNEP/MAP – Barcelona Convention. Athens.

UNEP/MAP/Blue Plan, 2005. A Sustainable Future for the Mediterranean: the Blue Plan's Environment and Development Outlook. Earthscan, London, UK.

UNEP/MAP/Blue Plan, 2009. State of the Environment and Development in the Mediterranean. UNEP/MAP Blue Plan, Athens.

UNEP/MAP/MED POL, 2011a. Diagnosis of Mercury in the Mediterranean Countries. UNEP/MAP/MED POL, Athens.

UNEP/MAP/MED POL, 2011b. Reviewing MED POL Marine Monitoring Activities and Planning for the New Integrated Map Monitoring System. UNEP/MAP/MED POL, Athens.

Warnau, M., Fowler, S.W., Teyssie, J.L., 1996. Biokinetics of selected heavy metals and radionuclides in two marine macrophytes: the seagrass *Posidonia oceanica* and the alga *Caulerpa taxifolia*. Mar. Environ. Res. 41 (4), 343–362.

Wilson, S., 2004. Development of Rehabilitation Strategies - Maghtab, Qortin and Wied Fulija Landfills. WasteServ Malta Ltd., Malta.

Wunsch, A., Navarre-Sitchler, A.K., Moore, J., Ricko, A., McCray, J.E., 2013. Metal release from dolomites at high partial-pressures of CO_2. Appl. Geochem. 38 (0), 33–47.

Wunsch, A., Navarre-Sitchler, A.K., Moore, J., McCray, J.E., 2014. Metal release from limestones at high partial-pressures of CO_2. Chem. Geol. 363, 40–55.

Zhou, Q.F., Zhang, J.B., Fu, J.J., Shi, J.B., Jiang, G.B., 2008. Biomonitoring: an appealing tool for assessment of metal pollution in the aquatic ecosystem. Anal. Chim. Acta 606 (2), 135–150.

Sampling area	Site name	Ref.	GPS coordinates		Site nb	Ag	As	Cd	Cu	Hg	Ni	Pb	TEPI
			North	East		mean ± SD	mean ± SD	mean ± SD	mean ± SD	mean ± SD	mean ± SD	mean ± SD	
Western Mediterranean basin													
Sub-area I - European continental coasts													
Spain													
	Alicante		38.251947	359.487600	1	0.167 ± 0.058	1.733 ± 0.379	0.93 ± 0.18	5.47 ± 0.85	0.1098 ± 0.0163	13.6 ± 1.0	2.17 ± 1.77	0.730
	Mont Roig		41.030150	0.971200	2	0.833 ± 0.058	0.500 ± 0.100	2.98 ± 0.13	12.80 ± 0.72	0.0800	19.9 ± 2.9	4.43 ± 1.01	1.146
	Torrembarra		41.146983	1.426717	3	0.400 ± 0.000	0.833 ± 0.058	2.26 ± 0.26	10.20 ± 1.15	0.0588 ± 0.0055	19.6 ± 1.6	1.70 ± 0.17	0.860
	Mataro		41.520283	2.451475	4	0.767 ± 0.115	0.833 ± 0.231	4.17 ± 0.38	15.27 ± 1.03	0.0500 ; 0.0600	25.1 ± 2.2	2.43 ± 0.59	1.178
	Medes		42.048889	3.219167	5	0.100 ± 0.000	1.333 ± 0.252	2.00 ± 0.16	6.73 ± 1.40	0.0638 ± 0.0059	19.5 ± 0.8	1.07 ± 0.06	0.661
France													
	Ensuès		43.329017	5.206567	6	0.562 ± 0.115	3.762 ± 0.525	1.99 ± 0.12	10.05 ± 0.67	ND	36.5 ± 1.8	3.21 ± 0.23	1.348
	La Vesse		43.340100	5.262467	7	1.364 ± 0.104	2.574 ± 0.374	2.35 ± 0.11	17.41 ± 1.12	ND	42.7 ± 4.2	6.08 ± 0.74	1.799
	Corbière		43.355400	5.296000	8	0.894 ± 0.167	2.815 ± 0.270	1.49 ± 0.11	17.15 ± 1.84	ND	35.0 ± 3.6	6.12 ± 1.12	1.560
	Marseille Cortiou		43.196717	5.370533	9	0.500 ± 0.173	1.233 ± 0.058	2.14 ± 0.19	9.97 ± 0.38	0.0683 ± 0.0029	20.7 ± 1.0	3.23 ± 0.55	1.047
	Riou		43.181983	5.378400	10	0.704 ± 0.114	2.014 ± 0.218	2.95 ± 0.20	9.28 ± 1.06	ND	42.5 ± 1.7	1.82 ± 0.28	1.255
	Toulon		43.099644	5.931139	11	0.400 ± 0.000	2.200 ± 0.265	1.81 ± 0.24	15.73 ± 1.19	0.1167 ± 0.0153	20.0 ± 1.4	5.57 ± 0.51	1.334
	Bénat		43.085167	6.351700	12	0.954 ± 0.193	1.463 ± 0.144	3.21 ± 0.36	11.25 ± 2.16	ND	45.1 ± 6.3	1.83 ± 0.20	1.315
	Giens		43.005783	6.441133	13	0.749 ± 0.025	1.154 ± 0.078	3.35 ± 0.19	10.56 ± 1.07	ND	45.9 ± 2.2	2.28 ± 0.27	1.267
	Cavalaire ZRC		43.178500	6.540380	14	0.500 ± 0.000	1.300 ± 0.173	2.78 ± 0.61	13.50 ± 5.34	0.0773 ± 0.0126	26.2 ± 1.5	8.57 ± 2.91	1.384
	St Raphaël		43.422933	6.898933	15	0.719 ± 0.089	1.336 ± 0.136	4.67 ± 0.48	10.37 ± 1.63	ND	66.0 ± 5.6	1.52 ± 0.26	1.336
	Cap Roux		43.446933	6.917033	16	0.551 ± 0.043	2.152 ± 0.167	3.05 ± 0.26	8.07 ± 0.73	ND	46.7 ± 4.0	1.77 ± 0.14	1.217
	Antibes		43.557133	7.143167	17	0.736 ± 0.076	3.585 ± 0.669	2.29 ± 0.16	12.45 ± 1.28	ND	38.8 ± 3.4	1.80 ± 0.24	1.360
	Villefranche		43.699333	7.314533	18	0.745 ± 0.112	1.999 ± 0.208	1.22 ± 0.07	22.11 ± 1.23	ND	30.2 ± 3.8	5.48 ± 1.07	1.406
Italy													
	Livorno 3		43.605500	10.207583	19	ND	ND	3.39 ± 0.21	ND	0.0770 ± 0.0208	28.9 ± 1.1	1.40 ± 0.44	1.000
	Livorno 2		43.589800	10.250067	20	ND	ND	2.38 ± 0.12	ND	0.0670 ± 0.0066	38.9 ± 9.8	1.43 ± 0.38	0.976
	Livorno 1		43.569517	10.261417	21	ND	ND	2.49 ± 0.06	ND	0.0723 ± 0.0129	33.7 ± 9.7	1.20 ± 0.10	0.948
	Livorno 4		43.547200	10.173567	22	ND	ND	3.63 ± 0.19	ND	0.0853 ± 0.0174	36.4 ± 3.6	1.13 ± 0.38	1.028
	Rosignano		43.363717	10.418583	23	ND	ND	3.40 ± 0.16	ND	0.1257 ± 0.0049	35.0 ± 2.2	1.27 ± 0.23	1.087
	Piombino		42.915025	10.519067	24	0.933 ± 0.058	0.467 ± 0.058	2.82 ± 0.05	25.87 ± 3.02	0.0867 ± 0.0153	35.1 ± 3.7	1.97 ± 0.61	1.235
	Torre Mozza		42.946567	10.694533	25	1.533 ± 0.153	0.633 ± 0.115	2.00 ± 0.20	20.70 ± 0.70	0.0893 ± 0.0058	17.3 ± 0.2	3.80 ± 0.10	1.274
	Talamone		42.559624	11.157310	26	0.633 ± 0.058	0.600 ± 0.100	1.90 ± 0.10	10.90 ± 0.40	0.1325 ± 0.0190	26.0 ± 4.3	1.73 ± 0.12	1.012
	Porto Ercole		42.436717	11.206133	27	<DL	1.033 ± 0.058	2.83 ± 0.24	17.27 ± 0.76	0.0503 ± 0.0101	6.1 ± 0.3	14.50 ± 1.90	0.824
	Santa Marinella		42.040267	11.894617	28	1.433 ± 0.208	0.300 ± 0.000	2.15 ± 0.38	11.10 ± 0.46	0.0659 ± 0.0102	22.3 ± 1.0	0.63 ± 0.06	0.805
	Lacco Ameno	(1)	40.753817	13.891842	29	0.233 ± 0.058	0.833 ± 0.058	1.89 ± 0.05	8.57 ± 0.46	0.0720 ± 0.0101	23.0 ± 0.6	1.60 ± 0.10	0.790
	Scarrupata	(1)	40.697056	13.916522	30	0.400 ± 0.000	0.467 ± 0.058	3.39 ± 0.15	10.03 ± 0.59	0.0558 ± 0.0094	33.7 ± 0.9	1.43 ± 0.29	0.876
	Agropoli		40.375783	15.001250	31	0.467 ± 0.058	0.733 ± 0.153	1.87 ± 0.24	13.57 ± 1.93	0.0468 ± 0.0028	31.5 ± 0.5	1.40 ± 0.10	0.882
Sub-area II - European insular coasts													
Baleares (Spain)													
	Mallorca		39.760083	3.406533	32	0.400 ± 0.000	0.367 ± 0.058	3.48 ± 0.13	7.47 ± 0.51	0.0965 ± 0.0077	22.9 ± 3.8	2.93 ± 0.15	0.923
Cosica (France)													
	Macinaggio	(1)	42.970440	9.465870	33	0.400 ± 0.000	0.467 ± 0.058	2.21 ± 0.30	6.93 ± 0.23	0.0507 ± 0.0078	19.8 ± 1.2	0.60 ± 0.26	0.631
	Sisco	(2)	42.813883	9.493233	34	ND	ND	3.89 ± 0.24	ND	0.0600 ± 0.0100	24.7 ± 0.7	2.63 ± 0.60	1.053
	Bastia	(2)	42.713100	9.458733	35	ND	ND	1.47 ± 0.10	ND	0.0713 ± 0.0006	19.6 ± 0.4	2.53 ± 0.15	0.904
	Toga	(1)	42.712990	9.457750	36	0.400 ± 0.000	0.400 ± 0.000	2.22 ± 0.18	7.93 ± 0.42	0.0684 ± 0.0109	21.3 ± 1.3	1.33 ± 0.06	0.744
	Arinella		42.668890	9.455470	37	0.333 ± 0.058	0.400 ± 0.000	1.94 ± 0.26	8.27 ± 1.31	0.0687 ± 0.0181	18.8 ± 2.8	1.60 ± 0.10	0.721
	Taglio Isolaccio		42.418533	9.552967	38	0.463 ± 0.049	1.376 ± 0.292	2.54 ± 0.15	8.75 ± 0.88	ND	38.1 ± 1.2	1.76 ± 0.13	1.065
	Campoloro	(2)	42.346167	9.542767	39	ND	ND	2.26 ± 0.11	ND	0.0567 ± 0.0058	21.1 ± 0.8	1.97 ± 0.06	0.907
	Bravone		42.201683	9.569267	40	1.020 ± 0.081	1.245 ± 0.109	2.63 ± 0.09	22.62 ± 2.61	ND	40.4 ± 2.1	3.47 ± 0.60	1.503
	Diane		42.116667	9.566667	41	0.267 ± 0.058	0.500 ± 0.100	2.45 ± 0.05	7.40 ± 0.26	0.0849 ± 0.0072	22.6 ± 1.0	0.83 ± 0.75	0.708
	Solenzara	(2)	41.862467	9.409317	42	ND	ND	2.58 ± 0.19	ND	0.0667 ± 0.0058	17.8 ± 1.1	2.20 ± 0.61	0.938
	La Chiappa	(1)	41.589740	9.368400	43	0.367 ± 0.058	0.467 ± 0.058	1.40 ± 0.23	9.17 ± 2.03	0.0645 ± 0.0017	24.6 ± 1.9	1.63 ± 0.06	0.748
	Sant'Amanza	(2)	41.409956	9.226325	44	ND	ND	1.52 ± 0.13	ND	0.0667 ± 0.0115	17.3 ± 1.1	1.27 ± 0.06	0.800
	Bonifacio	(2)	41.389117	9.147894	45	ND	ND	2.14 ± 0.14	ND	0.0433 ± 0.0058	22.3 ± 1.1	1.70 ± 0.26	0.855
	Propriano	(2)	41.690806	8.878625	46	ND	ND	2.17 ± 0.25	ND	0.0710 ± 0.0056	17.9 ± 2.5	1.40 ± 0.17	0.866
	Porto-Pollo		41.736480	8.766910	47	0.300 ± 0.000	0.367 ± 0.058	3.13 ± 0.12	6.97 ± 0.12	0.0723 ± 0.0118	30.9 ± 0.3	1.87 ± 0.06	0.811
	Ajaccio	(2)	41.882533	8.779506	48	ND	ND	3.53 ± 0.31	ND	0.0477 ± 0.0065	23.4 ± 0.9	3.37 ± 0.50	1.033
	Ajaccio Sud		41.890267	8.796433	49	0.831 ± 0.078	2.546 ± 0.215	2.63 ± 0.28	8.25 ± 0.41	ND	42.4 ± 2.1	3.13 ± 0.53	1.388
	Ajaccio Nord		41.905050	8.701700	50	0.405 ± 0.060	2.069 ± 0.191	1.75 ± 0.05	6.85 ± 0.30	ND	26.3 ± 1.9	5.91 ± 0.79	1.143
	La Parata		41.898450	8.622080	51	0.267 ± 0.058	0.500 ± 0.000	2.11 ± 0.04	6.30 ± 0.10	0.0600 ± 0.0100	20.3 ± 0.3	0.67 ± 0.40	0.615
	Sagone		42.103530	8.674880	52	0.400 ± 0.000	0.333 ± 0.058	3.42 ± 0.04	9.00 ± 0.10	0.0782 ± 0.0100	28.8 ± 1.0	1.67 ± 0.06	0.863
	Porto		42.260650	8.659570	53	0.467 ± 0.058	0.300 ± 0.000	4.43 ± 0.53	9.90 ± 0.26	0.0658 ± 0.0115	33.6 ± 3.0	5.33 ± 1.19	1.076
	Calvi Punta Bianca		42.569033	8.714283	54	0.567 ± 0.058	0.733 ± 0.115	4.52 ± 0.62	14.97 ± 4.55	0.0300	44.6 ± 11.4	3.77 ± 0.93	1.184

Sampling area	Site name	Ref.	GPS coordinates		Site nb	Ag	As	Cd	Cu	Hg	Ni	Pb	TEPI
			North	East		mean ± SD	mean ± SD	mean ± SD	mean ± SD	mean ± SD	mean ± SD	mean ± SD	
	Calvi Stareso		42.580750	8.725783	55	0.300 ± 0.000	0.467 ± 0.058	1.15 ± 0.06	8.33 ± 2.84	0.0483 ± 0.0027	23.3 ± 1.5	1.63 ± 0.25	0.664
	Calvi fishfarm		42.563131	8.766233	56	0.367 ± 0.058	0.333 ± 0.058	4.62 ± 0.32	9.07 ± 0.75	0.0200	36.2 ± 2.0	2.40 ± 0.10	0.798
	Lumio	(2)	42.598469	8.806967	57	ND	ND	2.13 ± 0.23	ND	0.0593 ± 0.0075	28.8 ± 4.7	1.30 ± 0.20	0.892
	Aregno		42.614250	8.868767	58	0.642 ± 0.028	1.054 ± 0.019	4.40 ± 0.10	13.59 ± 1.35	ND	40.4 ± 1.9	1.45 ± 0.08	1.213
	Ile Rousse	(1)	42.645620	8.937430	59	1.800 ; 1.300	0.400 ; 0.400	3.28 ; 3.35	11.20 ; 10.10	0.0470 ± 0.0013	21.1 ; 21.9	1.70 ; 1.70	0.980
	St Florent		42.689783	9.284983	60	0.408 ± 0.034	1.008 ± 0.119	1.89 ± 0.11	8.08 ± 1.22	ND	31.6 ± 2.8	3.00 ± 0.61	0.996
	Canari	(1)	42.784910	9.339740	61	0.633 ± 0.058	0.200 ± 0.000	4.29 ± 0.23	15.10 ± 0.70	0.0580 ± 0.0082	123.0 ± 8.0	2.97 ± 0.06	1.219
	Centuri	(2)	42.961525	9.347047	62	ND	ND	2.78 ± 0.14	ND	0.0487 ± 0.0023	27.7 ± 1.7	1.67 ± 0.15	0.928
	Sardinia (Italy)												
	Olbia		41.000444	9.621306	63	0.467 ± 0.058	0.367 ± 0.058	1.74 ± 0.30	27.70 ± 3.57	0.0646 ± 0.0047	14.4 ± 1.9	1.63 ± 0.25	0.838
	Tavolara		40.849633	9.692300	64	0.300 ± 0.000	1.200 ± 0.100	2.52 ± 0.08	7.03 ± 0.45	0.0647 ± 0.0065	24.2 ± 1.2	3.23 ± 0.06	0.959
	Cagliari 2		39.207083	9.302083	65	0.367 ± 0.058	0.533 ± 0.153	2.32 ± 0.13	5.40 ± 2.21	0.0764 ± 0.0046	18.6 ± 1.4	0.87 ± 0.06	0.683
	Cagliari 1		39.222444	9.239306	66	0.367 ± 0.058	0.267 ± 0.058	1.89 ± 0.16	4.30 ± 0.17	0.0769 ± 0.0042	16.4 ± 0.8	1.27 ± 0.21	0.604
	Oristano		39.833042	8.553292	67	0.083 ± 0.029	2.000 ± 0.529	0.38 ± 0.04	4.20 ± 1.18	0.0468 ± 0.0086	2.3 ± 0.3	2.93 ± 0.15	0.411
	Bosa		40.284808	8.474883	68	0.200 ± 0.000	0.833 ± 0.115	0.95 ± 0.01	5.87 ± 0.81	0.0557 ± 0.0050	12.5 ± 0.8	2.67 ± 0.47	0.631
	Alghero		40.580044	8.309533	69	0.667 ± 0.058	0.367 ± 0.153	1.80 ± 0.37	18.27 ± 2.81	0.0569 ± 0.0089	15.7 ± 1.9	1.47 ± 0.40	0.818
	Porto Torres 4		41.051640	8.283140	70	ND	ND	1.96 ± 0.35	ND	0.0520 ± 0.0053	22.0 ± 1.2	2.00 ± 0.10	0.885
	Porto Torres 3		40.978640	8.239510	71	ND	ND	2.10 ± 0.18	ND	0.0583 ± 0.0032	27.5 ± 1.9	1.80 ± 0.00	0.924
	Porto Torres 2		40.869880	8.297720	72	ND	ND	2.68 ± 0.20	ND	0.1003 ± 0.0172	20.5 ± 1.0	2.73 ± 0.57	1.052
	Porto Torres 1		40.850010	8.342690	73	ND	ND	2.83 ± 0.24	ND	0.0813 ± 0.0264	23.2 ± 0.3	2.37 ± 0.21	1.026
	Porto Torres 5		40.838728	8.417222	74	0.467 ± 0.058	0.700 ± 0.100	1.95 ± 0.16	7.80 ± 0.75	0.0878 ± 0.0097	15.5 ± 1.2	1.37 ± 0.55	0.802
Sub-area III - North African coasts													
	Spain												
	Chafarinas		35.180006	357.569414	75	<DL	0.800 ± 0.000	1.37 ± 0.05	13.43 ± 1.33	0.0429 ± 0.0053	12.7 ± 0.8	2.03 ± 0.21	0.567
	Algeria												
	Annaba		36.893456	7.779814	76	0.267 ± 0.058	0.867 ± 0.115	1.81 ± 0.08	5.17 ± 0.38	0.0695 ± 0.0138	13.6 ± 2.4	3.60 ± 0.46	0.776
	Tunisia												
	Tabarka		36.954744	8.767150	77	0.233 ± 0.058	1.133 ± 0.208	2.13 ± 0.13	4.87 ± 1.17	0.0777 ± 0.0054	17.8 ± 2.0	2.33 ± 0.68	0.797
	La Galite		37.536801	8.938876	78	0.300 ± 0.000	0.800 ± 0.000	2.06 ± 0.15	12.00 ± 0.82	0.0489 ± 0.0088	18.9 ± 1.1	2.93 ± 0.72	0.868
	Sidi Mechreg		37.164717	9.122424	79	0.400 ± 0.000	1.233 ± 0.586	3.23 ± 0.14	9.20 ± 0.36	0.0923 ± 0.0149	10.8 ± 2.4	1.07 ± 0.06	0.864
	Sidi Ali el Mekki		37.186767	10.269333	80	0.167 ± 0.058	0.933 ± 0.058	2.44 ± 0.19	3.20 ± 0.56	0.0502 ± 0.0099	17.4 ± 1.8	2.33 ± 0.85	0.665
	Salammbó		36.842767	10.327819	81	0.775 ± 0.220	0.442 ± 0.032	2.97 ± 0.10	8.96 ± 3.78	0.1280 ± 0.0474	30.7 ± 4.2	5.93 ± 2.77	1.254
	Zembra		37.136125	10.808897	82	0.300 ± 0.000	1.800 ± 0.000	1.79 ± 0.04	7.57 ± 0.25	0.0480 ± 0.0003	14.7 ± 0.2	1.57 ± 0.06	0.787
Eastern Mediterranean basin													
Sub-area IV - western coasts													
	Tunisia												
	Monastir		35.775128	10.843294	83	0.133 ± 0.058	0.600 ± 0.000	0.37 ± 0.02	1.87 ± 0.06	0.0435 ± 0.0029	1.6 ± 0.2	0.70 ± 0.00	0.251
	Kerkena		34.681514	11.113286	84	<DL	0.600 ± 0.100	1.24 ± 0.19	4.37 ± 0.67	0.0480 ± 0.0088	12.1 ± 0.3	1.23 ± 0.42	0.429
	Libya												
	Tajura		32.897528	13.355822	85	0.433 ± 0.058	0.500 ± 0.173	2.55 ± 0.19	3.27 ± 0.38	0.0630 ± 0.0087	14.0 ± 2.1	1.30 ± 0.30	0.648
	Garabouilli		32.814530	13.705220	86	0.200 ± 0.000	0.433 ± 0.058	2.31 ± 0.30	3.90 ± 1.18	0.0892 ± 0.0191	11.4 ± 0.3	1.03 ± 0.12	0.567
	Malta												
	Rdum il-Kbir		36.065017	14.296233	87	0.200 ± 0.000	0.200 ± 0.000	2.58 ± 0.04	6.90 ± 0.10	0.0948 ± 0.0081	15.5 ± 0.8	7.90 ± 0.30	0.790
	Dahlet ix-Xmajjar		35.998983	14.366783	88	0.167 ± 0.058	0.567 ± 0.058	2.48 ± 0.04	5.63 ± 0.61	0.0504 ± 0.0007	14.6 ± 0.1	3.37 ± 0.25	0.692
	St Paul's Bay		35.954783	14.392733	89	<DL	0.133 ± 0.058	1.42 ± 0.06	3.57 ± 0.15	0.0513 ± 0.0074	15.4 ± 0.4	4.60 ± 0.66	0.433
	Bahar ic-Caghaq		35.953650	14.448467	90	0.333 ± 0.058	0.167 ± 0.058	3.45 ± 0.19	6.93 ± 0.06	0.1063 ± 0.0124	20.2 ± 0.5	4.07 ± 0.42	0.829
	Qalet Marku Bay		35.949267	14.453017	91	0.200 ± 0.000	0.400 ± 0.000	2.52 ± 0.04	5.50 ± 0.10	0.0556 ± 0.0082	20.2 ± 0.7	1.73 ± 0.06	0.652
	Marsaxlokk Bay		35.828633	14.547200	92	0.400 ± 0.000	0.300 ± 0.000	1.42 ± 0.01	23.00 ± 0.50	0.0616 ± 0.0072	14.4 ± 0.3	1.43 ± 0.06	0.734
	Italy												
	Gallipoli		40.057417	17.976183	93	0.367 ± 0.058	1.100 ± 0.100	1.21 ± 0.05	16.43 ± 1.42	0.0621 ± 0.0077	22.1 ± 1.6	1.77 ± 0.64	0.892
	Torre San Giovanni		39.897350	18.097500	94	0.233 ± 0.058	0.267 ± 0.058	2.60 ± 0.40	6.97 ± 0.65	0.0622 ± 0.0062	33.1 ± 1.6	0.83 ± 0.06	0.641
Sub-area V - Adriatic coasts													
	Croatia												
	Island Vlasnik	(3)	42.753353	16.796739	95	0.167 ± 0.058	0.667 ± 0.058	2.75 ± 0.25	6.20 ± 0.26	0.0658 ± 0.0063	22.6 ± 6.1	0.77 ± 0.25	0.652
	Seget Donji	(3)	43.511983	16.213789	96	0.233 ± 0.058	0.333 ± 0.058	1.72 ± 0.06	10.57 ± 0.55	0.0942 ± 0.0198	20.8 ± 2.4	1.33 ± 0.06	0.704
	Lavdara	(3)	43.948000	15.198533	97	0.100 ± 0.000	1.767 ± 0.379	1.41 ± 0.03	4.73 ± 0.15	0.0538 ± 0.0045	21.4 ± 1.1	0.90 ± 0.17	0.601
	Brbinjscica	(3)	44.055117	14.991983	98	0.300 ± 0.000	5.300 ± 0.608	2.44 ± 0.16	7.43 ± 0.57	0.0412 ± 0.0138	32.1 ± 1.2	1.23 ± 0.12	1.012
	Zadar	(3)	44.103583	15.235861	99	0.833 ± 0.058	0.400 ± 0.100	1.74 ± 0.18	15.17 ± 0.55	0.0741 ± 0.0151	18.4 ± 1.0	1.50 ± 0.26	0.882
	Slovenia												
	Izola	(3)	45.548683	13.696233	100	0.133 ± 0.058	0.867 ± 0.058	2.10 ± 0.47	11.83 ± 0.38	0.0917 ± 0.0086	40.1 ± 3.6	1.50 ± 0.10	0.866

Sampling area	Site name	Ref.	GPS coordinates North	GPS coordinates East	Site nb	Ag mean ± SD	As mean ± SD	Cd mean ± SD	Cu mean ± SD	Hg mean ± SD	Ni mean ± SD	Pb mean ± SD	TEPI
Sub-area VI - Aegean-Levantine coasts													
Greece													
	Crete		35.399658	25.027119	101	0.067 ± 0.029	0.200 ± 0.000	2.72 ± 0.14	8.13 ± 0.57	0.0782 ± 0.0087	18.4 ± 1.3	1.17 ± 0.15	0.528
	Ligaria		35.401069	25.028414	102	<DL	0.500 ± 0.200	1.55 ± 0.19	6.07 ± 1.27	0.0754 ± 0.0055	10.5 ± 1.1	4.07 ± 0.67	0.561
	Kalogria		40.129519	23.760458	103	<DL	0.300 ± 0.000	2.73 ± 0.28	6.23 ± 0.12	0.0273 ± 0.0121	18.1 ± 0.7	1.17 ± 0.12	0.444
Turkey													
	Gokceada		40.224400	25.867894	104	0.167 ± 0.058	0.467 ± 0.058	4.40 ± 0.38	4.97 ± 0.25	0.0658 ± 0.0105	37.4 ± 2.1	3.90 ± 2.25	0.870
	Urla		38.360847	26.794650	105	<DL	0.567 ± 0.058	1.62 ± 0.15	2.17 ± 0.12	0.2041 ± 0.0072	9.3 ± 0.1	1.27 ± 0.06	0.476
	Turgutlar bay		36.154100	33.445267	106	<DL	1.233 ± 0.058	1.80 ± 0.07	5.17 ± 0.12	0.0793 ± 0.0034	21.3 ± 0.5	0.83 ± 0.06	0.566
	Mersin		36.790522	34.637447	107	<DL	0.967 ± 0.115	2.09 ± 0.07	7.87 ± 0.15	0.0932 ± 0.0110	20.8 ± 1.5	1.80 ± 0.26	0.675
Cyprus													
	Cape Greco		34.957158	34.085173	108	<DL	0.200 ± 0.000	4.14 ± 0.62	14.70 ± 1.65	0.0679 ± 0.0090	24.6 ± 0.2	1.17 ± 0.12	0.598
	Larnaca		34.870117	33.655133	109	<DL	0.400 ± 0.000	1.61 ± 0.19	21.17 ± 2.02	0.0867 ± 0.0130	22.8 ± 1.3	1.27 ± 0.23	0.630
Egypt													
	Alexandria		31.094064	29.692653	110	0.083 ± 0.029	0.367 ± 0.058	2.43 ± 0.17	6.60 ± 0.10	0.1264 ± 0.0064	23.8 ± 0.8	0.80 ± 0.10	0.597

Annex A

Trace element (TE) concentrations (mean ± SD, in µg g_{DW}^{-1}) measured in the blades of *Posidonia oceanica* adult leaves sampled between April and July of years 2003-2008 in 110 sites (numbers 1-110) located along the coasts of 13 Mediterranean countries. The Mediterranean was subdivided into 6 sub-areas (sub-areas I-VI), according to site location along its north-to-south and west-to-east axes. Site GPS coordinates (in Decimal Degrees, WGS 84) are given. Number of replicates n = 3-5, except for Hg in sites 2, 54, 56 (n = 1) and 4 (n = 2, given as individual measures) and for Ag, As, Cd, Cu, Ni and Pb in site 59 (n = 2, given as individual measures). <DL represent Ag concentrations below their analytical detection limit. ND = not determined. Site Trace Element Pollution Index (TEPI) values (no unit) were calculated from mean normalized TE concentrations. Data previously published have been associated with their respective reference: (1) Lopez y Royo et al., 2009; (2) Lafabrie et al., 2008; (3) Salivas-Decaux et al., 2009.

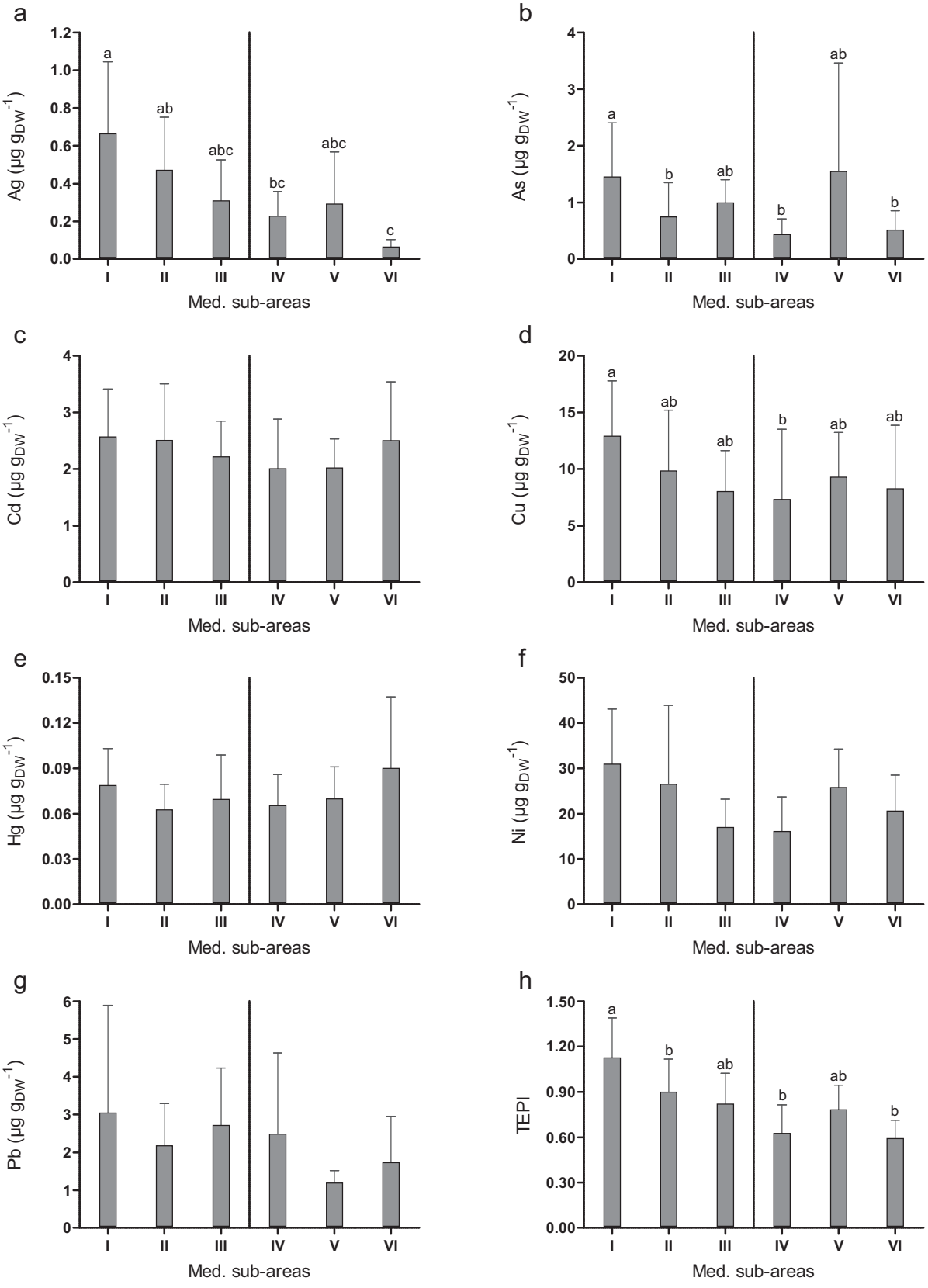

Annex B

a) Ag, b) As, c) Cd, d) Cu, e) Hg, f) Ni and g) Pb concentrations (mean ± SD, in µg g_{DW}^{-1}) measured in the blades of *Posidonia oceanica* adult leaves sampled between April and July of years 2003-2008 in 110 sites located along the coasts of 13 Mediterranean countries, and h) Trace Element Pollution Index (TEPI) values (mean ± SD, no unit) calculated from mean normalized trace element (TE) concentrations. The Mediterranean was subdivided into 6 sub-areas according to site location along its north-to-south and west-to-east axes. Sub-area I: European continental coasts (number of sites n = 31); sub-area II: European insular coasts (n = 43); sub-area III: North African coasts of the western Mediterranean (n = 8); sub-area IV: western coasts of the eastern Mediterranean (n = 12); sub-area V: Adriatic coasts (n = 6); sub-area VI: coasts of the Aegean-Levantine basin (n = 10). The full vertical line separates sub-areas of the western and the eastern Mediterranean, respectively. Letters represent significant ($p < 0.05$) differences between sub-areas.

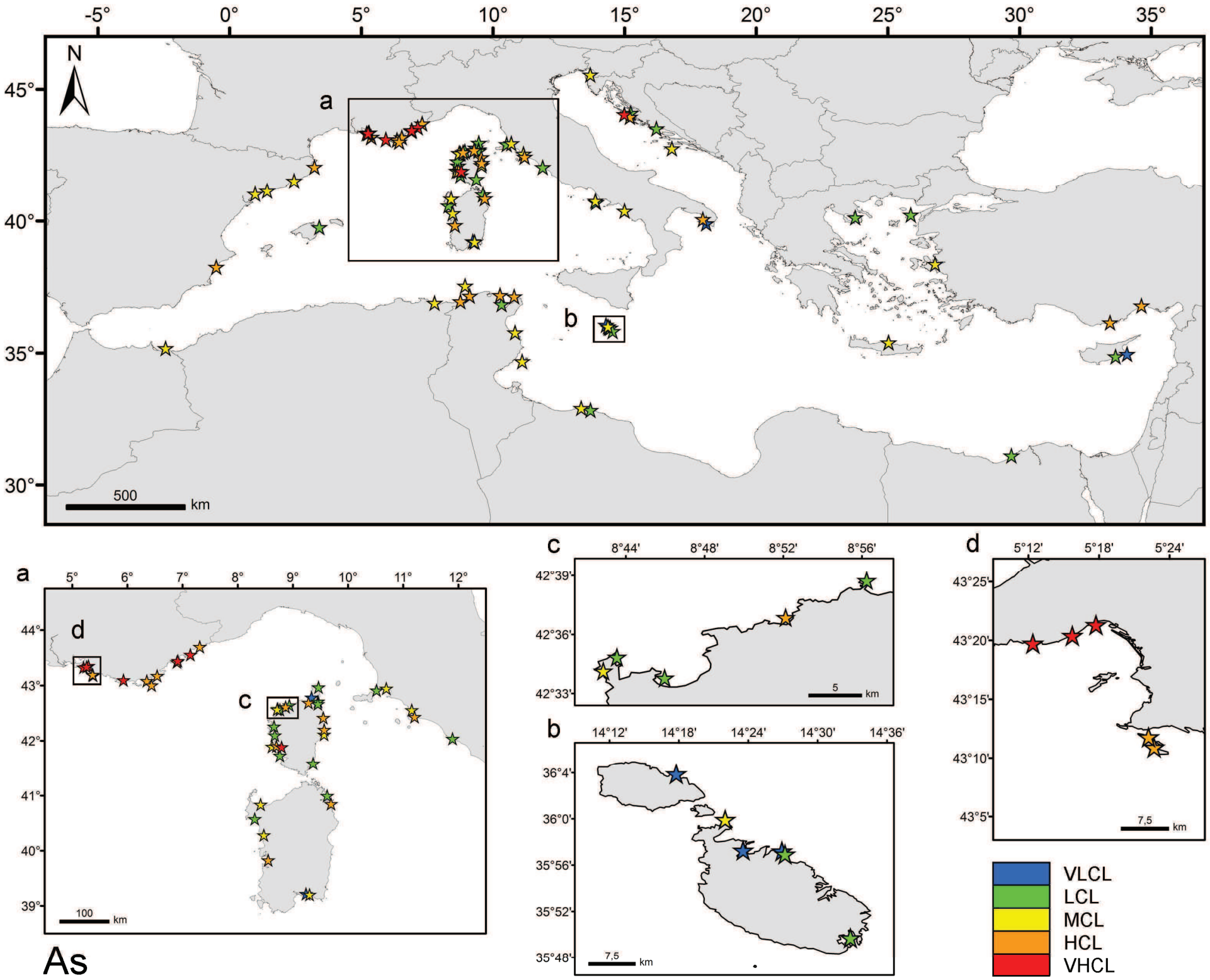
-5°
0°
5°
10°
15°
20°
25°
30°
35°
45°
40°
35°
30°
N
a
b
500
km
a
5°
6°
7°
8°
9°
10°
11°
12°
44°
43°
42°
41°
40°
39°
d
c
100
km
As
c
8°44'
8°48'
8°52'
8°56'
42°39'
42°36'
42°33'
5
km
b
14°12'
14°18'
14°24'
14°30'
14°36'
36°4'
36°0'
35°56'
35°52'
35°48'
7,5
km
d
5°12'
5°18'
5°24'
43°25'
43°20'
43°15'
43°10'
43°5'
7,5
km
VLCL
LCL
MCL
HCL
VHCL

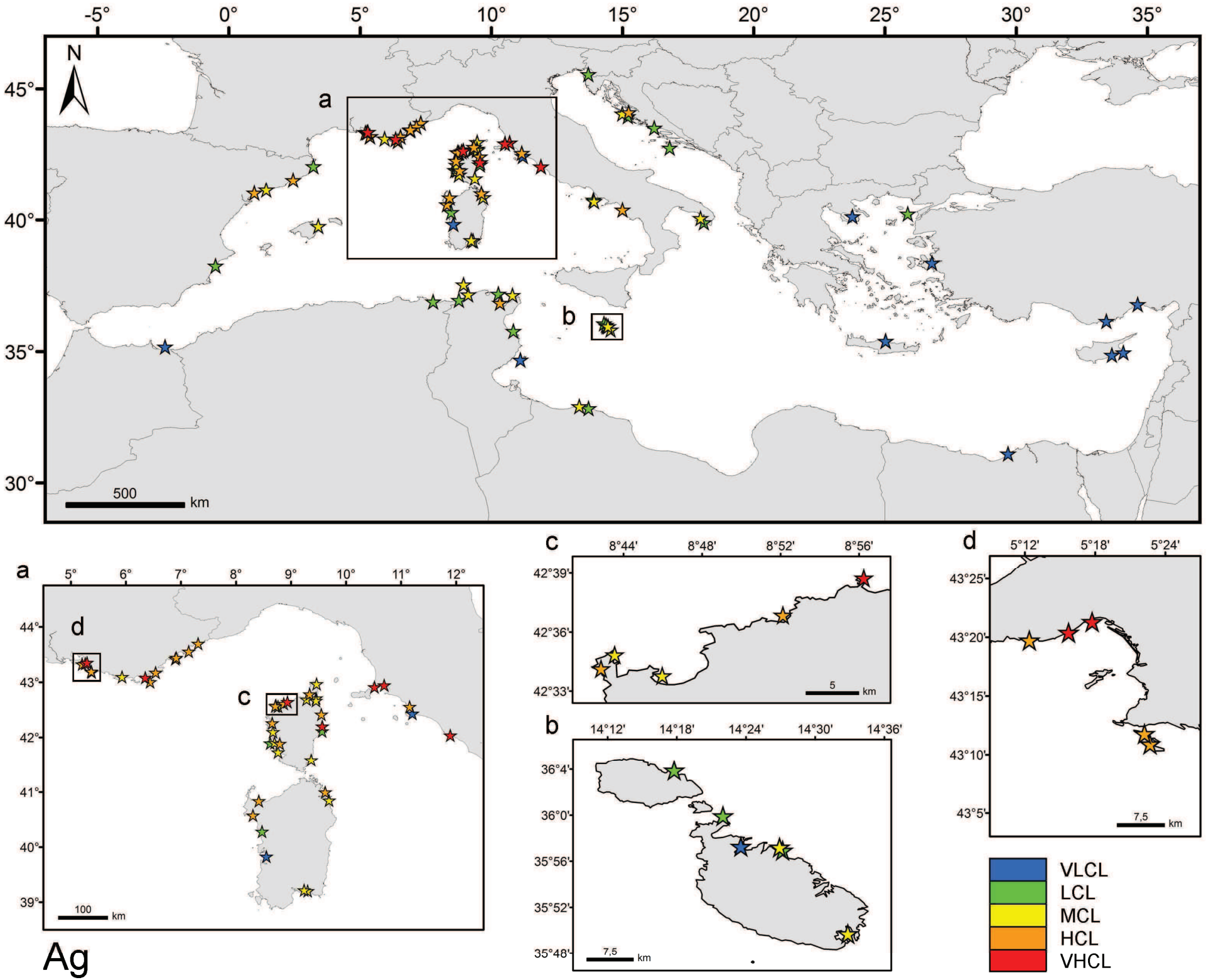
-5°
0°
5°
10°
15°
20°
25°
30°
35°
N
45°
40°
35°
30°
a
b
500
km
a
5°
6°
7°
8°
9°
10°
11°
12°
44°
43°
42°
41°
40°
39°
d
c
100
km
c
8°44'
8°48'
8°52'
8°56'
42°39'
42°36'
42°33'
5
km
b
14°12'
14°18'
14°24'
14°30'
14°36'
36°4'
36°0'
35°56'
35°52'
35°48'
7,5
km
d
5°12'
5°18'
5°24'
43°25'
43°20'
43°15'
43°10'
43°5'
7,5
km
VLCL
LCL
MCL
HCL
VHCL

Ag

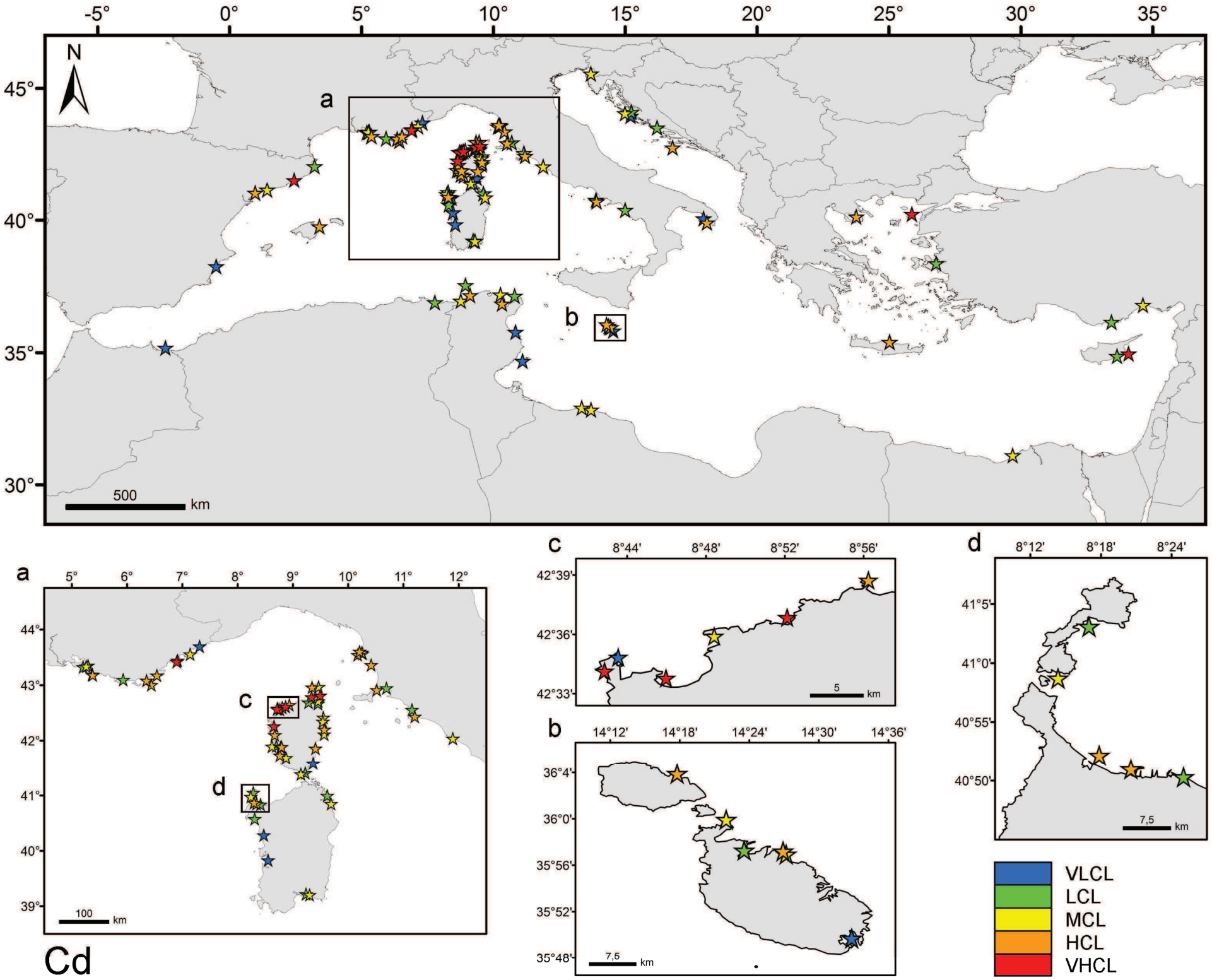
-5°
0°
5°
10°
15°
20°
25°
30°
35°
N
45°
40°
35°
30°
a
b
500
km
a
5°
6°
7°
8°
9°
10°
11°
12°
44°
43°
42°
41°
40°
39°
c
d
100
km
c
8°44'
8°48'
8°52'
8°56'
42°39'
42°36'
42°33'
5
km
b
14°12'
14°18'
14°24'
14°30'
14°36'
36°4'
36°0'
35°56'
35°52'
35°48'
7,5
km
d
8°12'
8°18'
8°24'
41°5'
41°0'
40°55'
40°50'
7,5
km
VLCL
LCL
MCL
HCL
VHCL

Cd

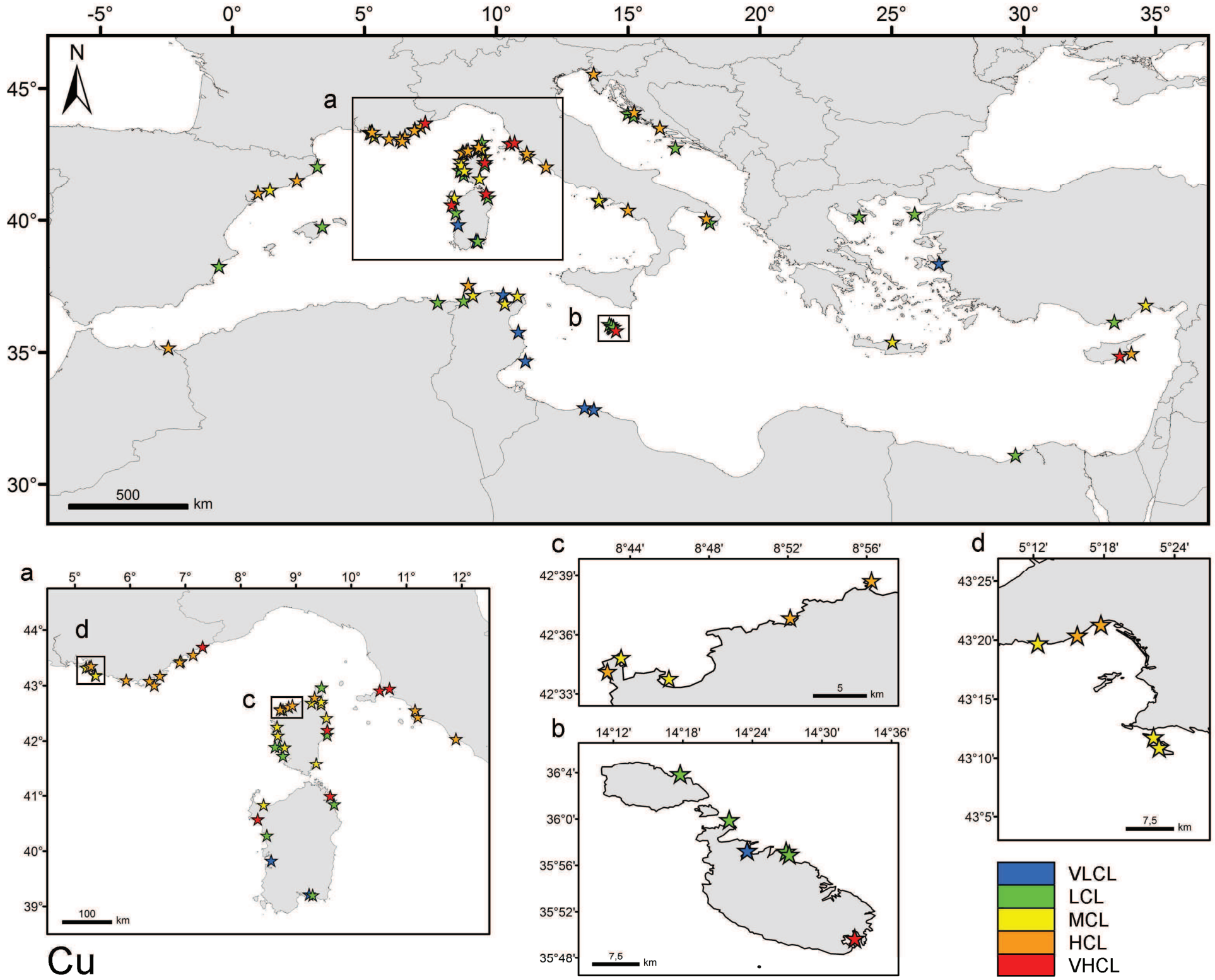
-5°
0°
5°
10°
15°
20°
25°
30°
35°
45°
40°
35°
30°
N
a
b
500
km
a
5°
6°
7°
8°
9°
10°
11°
12°
44°
43°
42°
41°
40°
39°
d
c
100
km
c
8°44'
8°48'
8°52'
8°56'
42°39'
42°36'
42°33'
5
km
b
14°12'
14°18'
14°24'
14°30'
14°36'
36°4'
36°0'
35°56'
35°52'
35°48'
7,5
km
d
5°12'
5°18'
5°24'
43°25'
43°20'
43°15'
43°10'
43°5'
7,5
km
VLCL
LCL
MCL
HCL
VHCL
Cu

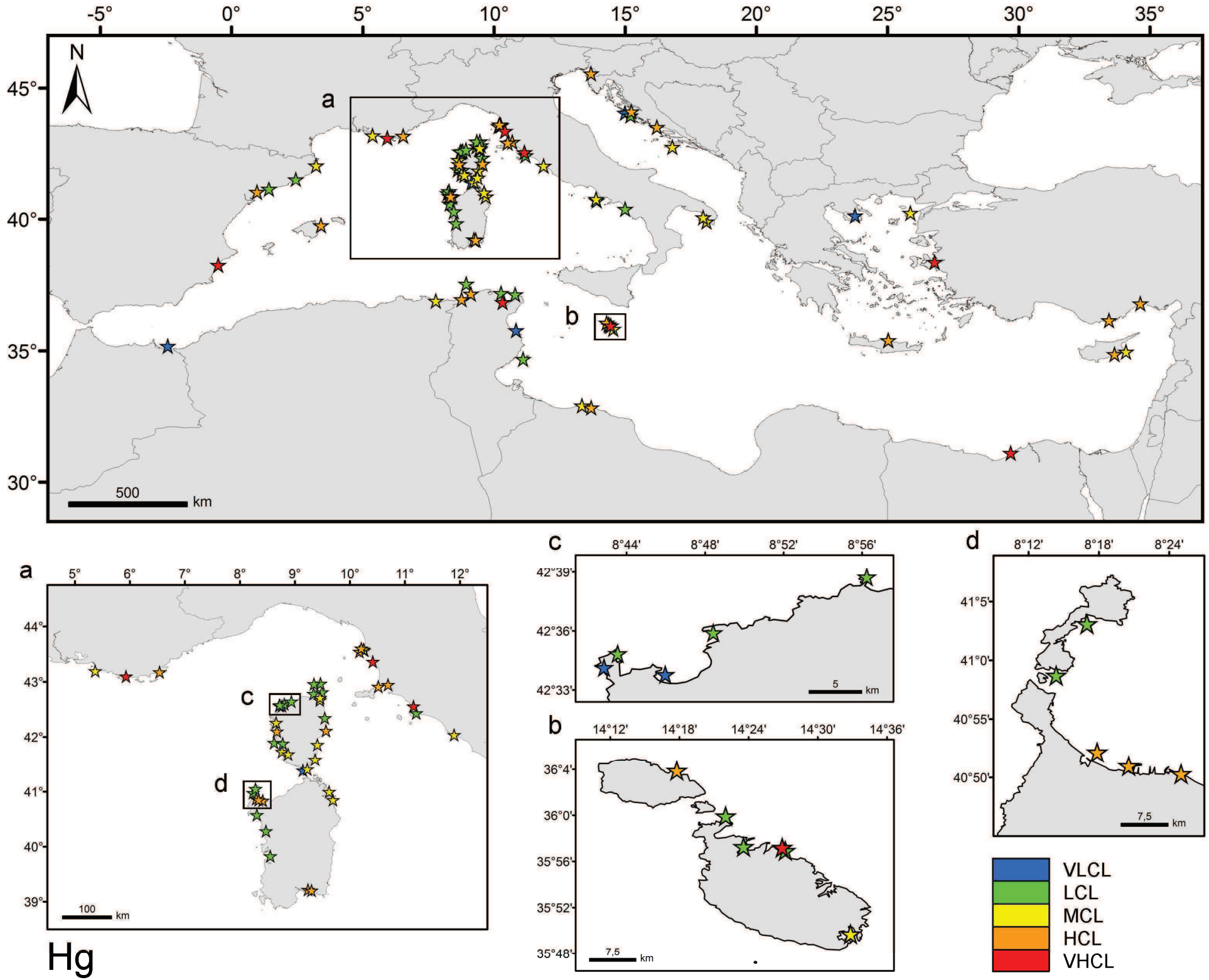
-5°
0°
5°
10°
15°
20°
25°
30°
35°
N
45°
40°
35°
30°
a
b
500
km
a
5°
6°
7°
8°
9°
10°
11°
12°
44°
43°
42°
41°
40°
39°
c
d
100
km
Hg
c
8°44'
8°48'
8°52'
8°56'
42°39'
42°36'
42°33'
5
km
b
14°12'
14°18'
14°24'
14°30'
14°36'
36°4'
36°0'
35°56'
35°52'
35°48'
7,5
km
d
8°12'
8°18'
8°24'
41°5'
41°0'
40°55'
40°50'
7,5
km
VLCL
LCL
MCL
HCL
VHCL

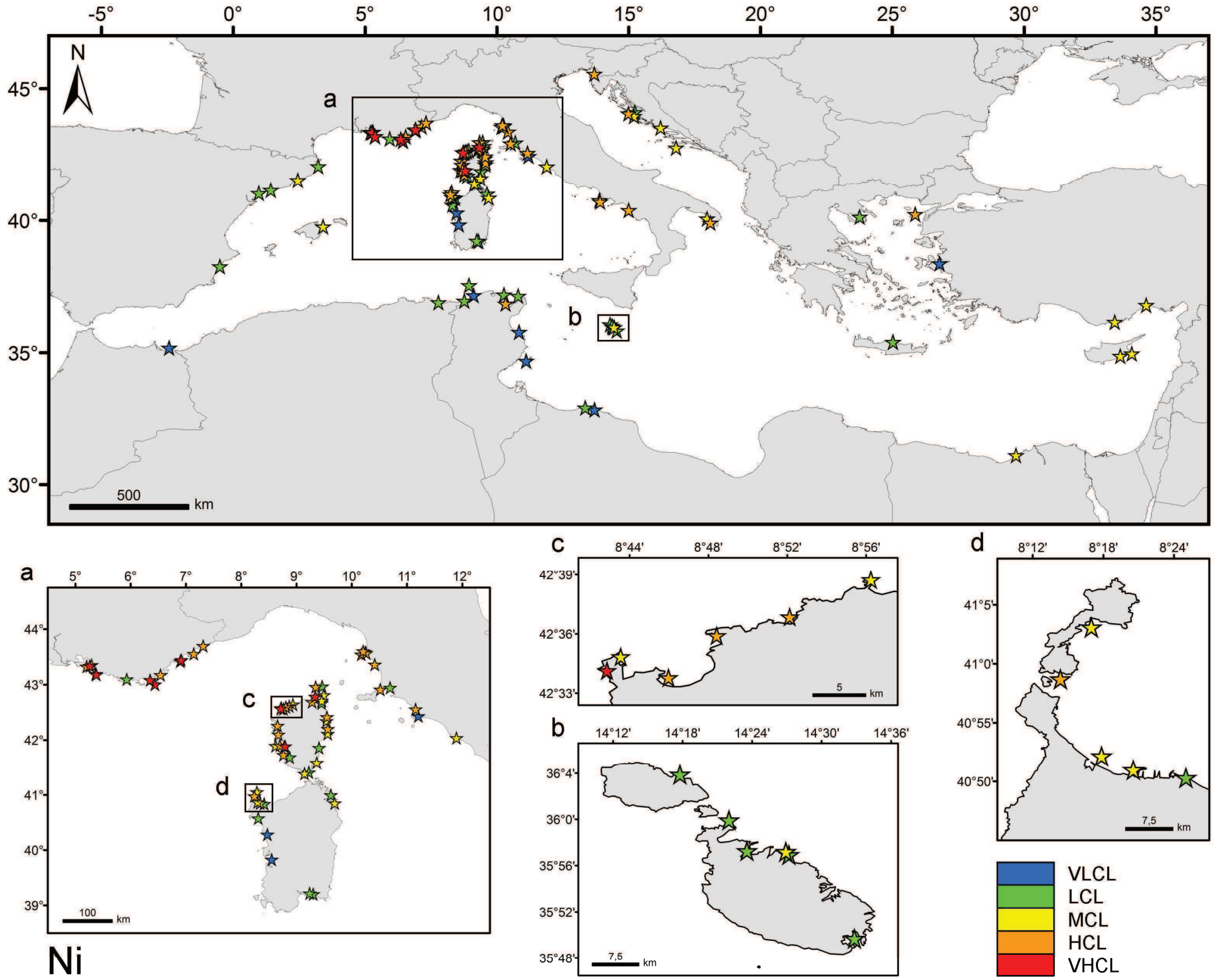
-5°
0°
5°
10°
15°
20°
25°
30°
35°
N
45°
40°
35°
30°
a
b
500
km
a
5°
6°
7°
8°
9°
10°
11°
12°
44°
43°
42°
41°
40°
39°
c
d
100
km
c
8°44'
8°48'
8°52'
8°56'
42°39'
42°36'
42°33'
5
km
b
14°12'
14°18'
14°24'
14°30'
14°36'
36°4'
36°0'
35°56'
35°52'
35°48'
7,5
km
d
8°12'
8°18'
8°24'
41°5'
41°0'
40°55'
40°50'
7,5
km
VLCL
LCL
MCL
HCL
VHCL
Ni

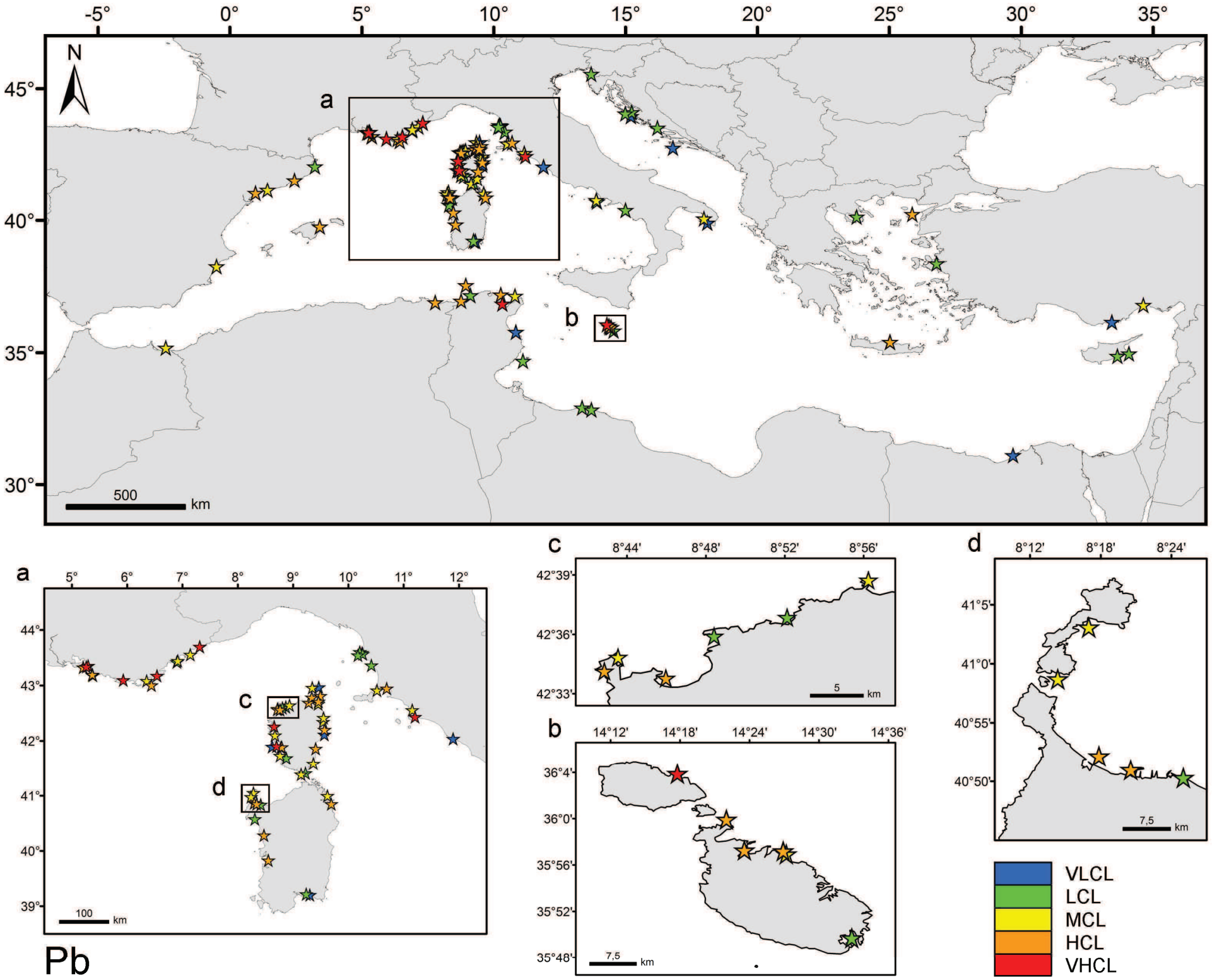
-5°
0°
5°
10°
15°
20°
25°
30°
35°
N
45°
40°
35°
30°
a
b
500
km
a
5°
6°
7°
8°
9°
10°
11°
12°
44°
43°
42°
41°
40°
39°
c
d
100
km
Pb
c
8°44'
8°48'
8°52'
8°56'
42°39'
42°36'
42°33'
5
km
b
14°12'
14°18'
14°24'
14°30'
14°36'
36°4'
36°0'
35°56'
35°52'
35°48'
7,5
km
d
8°12'
8°18'
8°24'
41°5'
41°0'
40°55'
40°50'
7,5
km
VLCL
LCL
MCL
HCL
VHCL

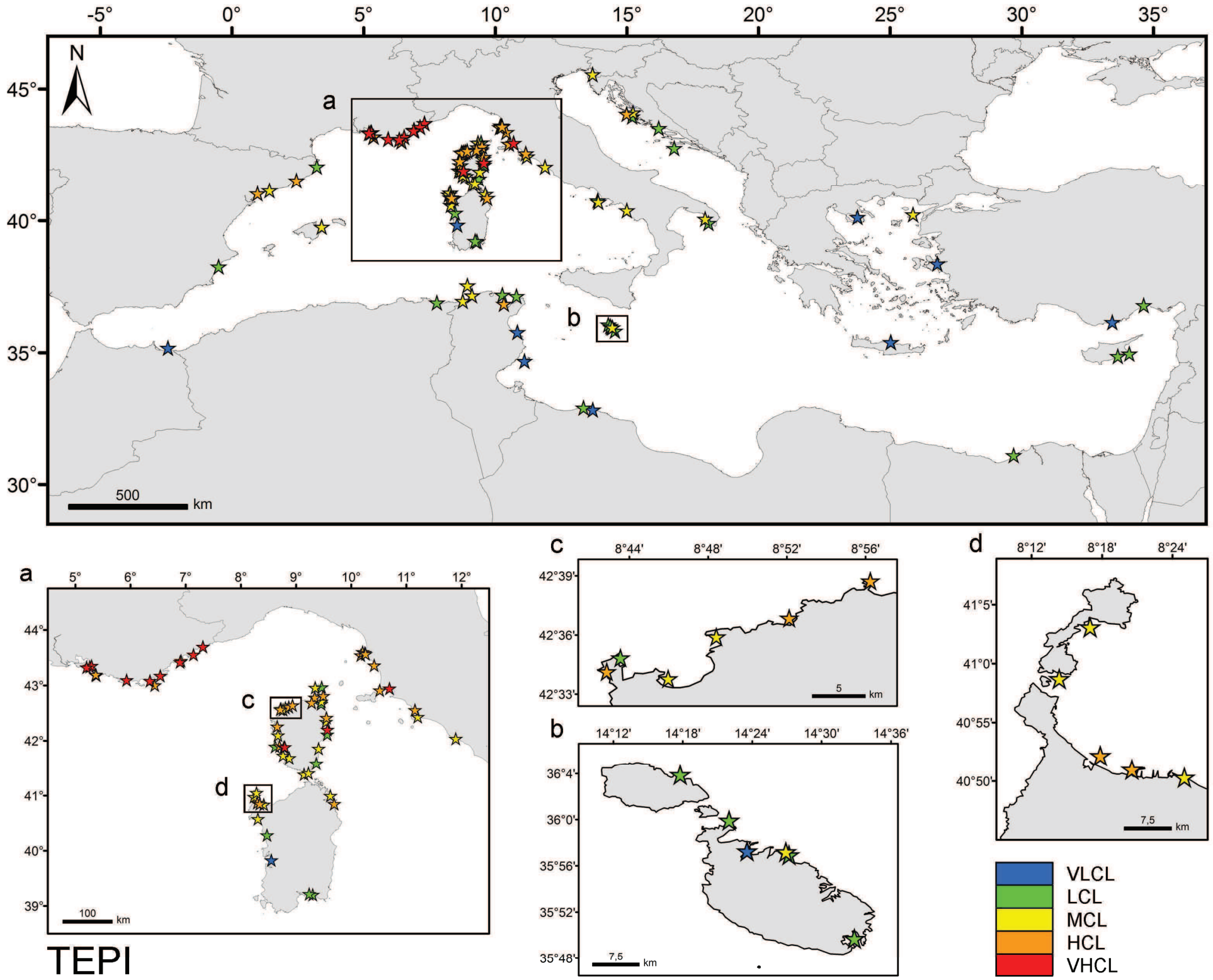
-5°
0°
5°
10°
15°
20°
25°
30°
35°
N
45°
40°
35°
30°
a
b
500
km
a
5°
6°
7°
8°
9°
10°
11°
12°
44°
43°
42°
41°
40°
39°
c
d
100
km
TEPI
c
8°44'
8°48'
8°52'
8°56'
42°39'
42°36'
42°33'
5
km
b
14°12'
14°18'
14°24'
14°30'
14°36'
36°4'
36°0'
35°56'
35°52'
35°48'
7,5
km
d
8°12'
8°18'
8°24'
41°5'
41°0'
40°55'
40°50'
7,5
km
VLCL
LCL
MCL
HCL
VHCL

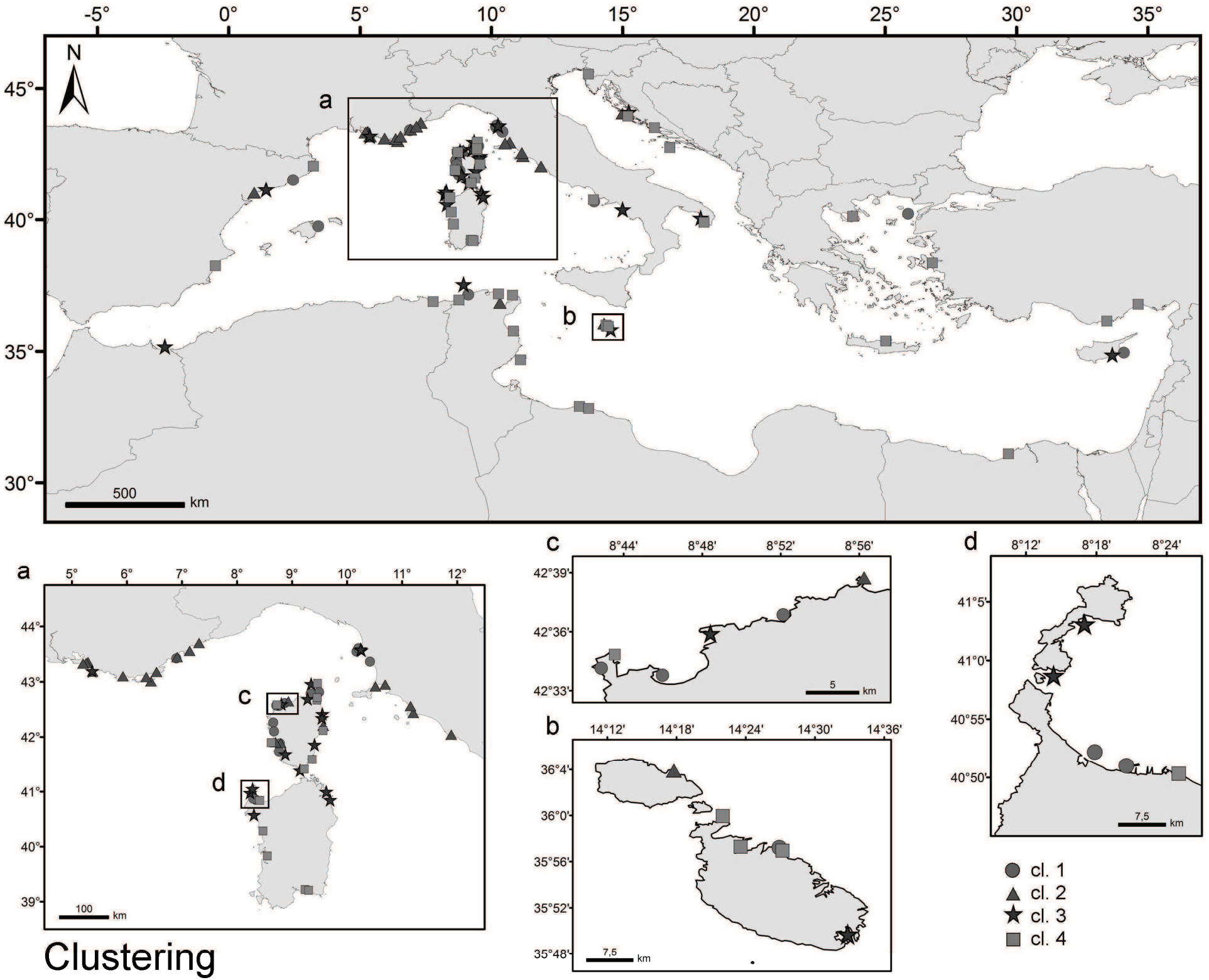
-5°
0°
5°
10°
15°
20°
25°
30°
35°
N
45°
40°
35°
30°
a
b
500
km
a
5°
6°
7°
8°
9°
10°
11°
12°
44°
43°
42°
41°
40°
39°
c
d
100
km
c
8°44'
8°48'
8°52'
8°56'
42°39'
42°36'
42°33'
5
km
b
14°12'
14°18'
14°24'
14°30'
14°36'
36°4'
36°0'
35°56'
35°52'
35°48'
7,5
km
d
8°12'
8°18'
8°24'
41°5'
41°0'
40°55'
40°50'
7,5
km
cl. 1
cl. 2
cl. 3
cl. 4
Clustering

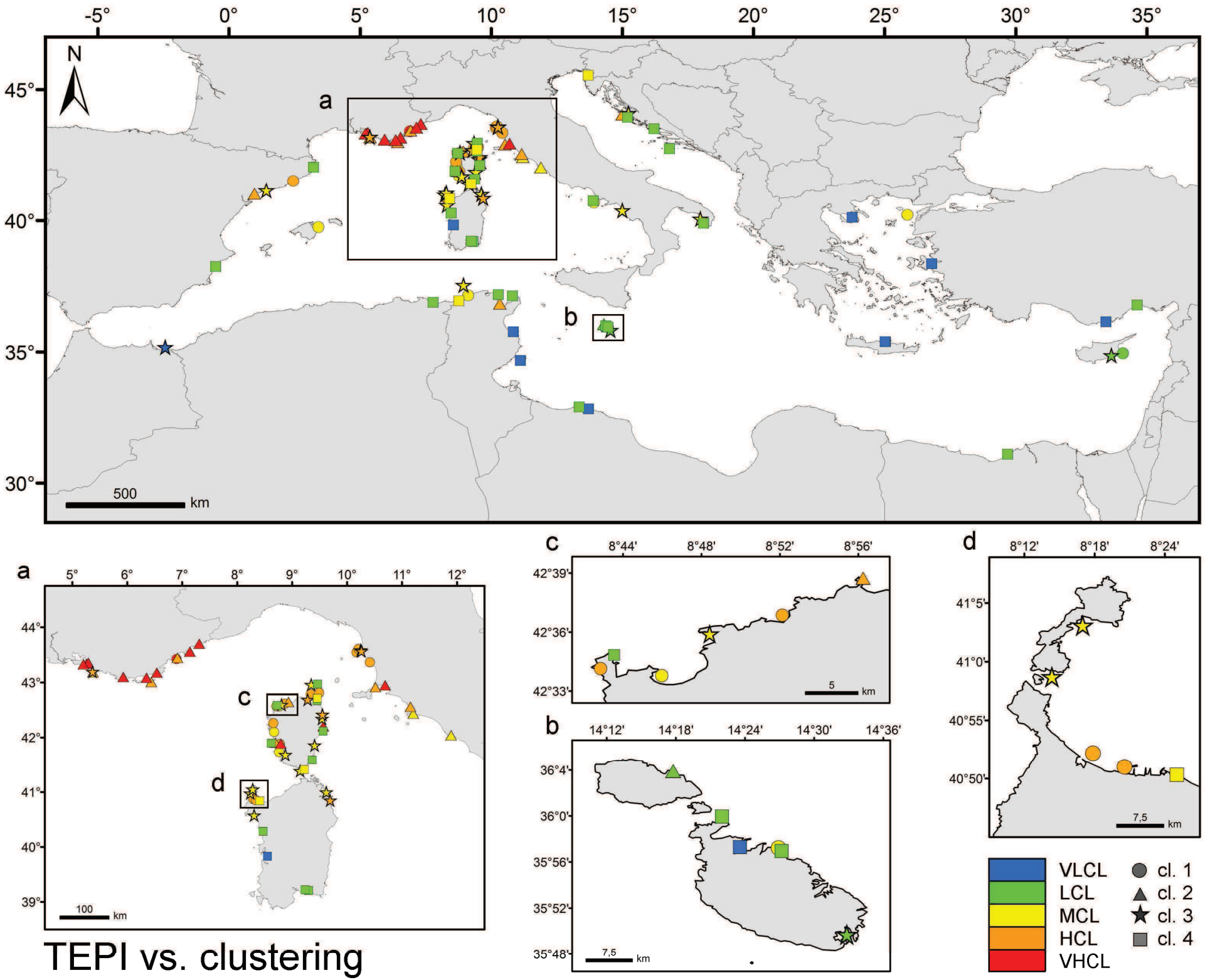

TEPI vs. clustering

Annex C

Maps of the contamination by Ag, As, Cd, Cu, Hg, Ni and Pb in 110 sites located along the coasts of 13 Mediterranean countries and map of the global contamination by these 7 trace elements (TEs), expressed as Trace Element Pollution Index (TEPI) values. TEPI values were calculated from mean normalized TE concentrations. TEs were measured in the blades of *Posidonia oceanica* adult leaves sampled between April and July of years 2003-2008. For clarity purpose, country names were not reported on maps (see Fig. 1). Site global or TE-specific contamination levels were GIS mapped according to a 5-level coastal water quality scale proposed using the quantile method, with contamination levels ranging from very low (VLCL, in blue) to very high (VHCL, in red; see Table 2). Sites were further clustered according to their contamination similarities (see Fig. 5 and Table 5) and each of the 4 resulting clusters (cl. 1-4) was symbolized by a geometric form. The synthesis map of the present study overlays the global TE contamination along Mediterranean coasts and contamination similarities among sites (*i.e.* TEPI vs. clustering). For clarity (site overlapping) and illustrative (different spatial scales) purposes, zooms were performed firstly on the northwestern Mediterranean area (zoomed area a; France and Italy) and on Malta (zoomed area b), and secondarily on the northwestern part of Corsica (zoomed area c) and Sardinia or eastern side of the Gulf of Lion (zoomed area d).

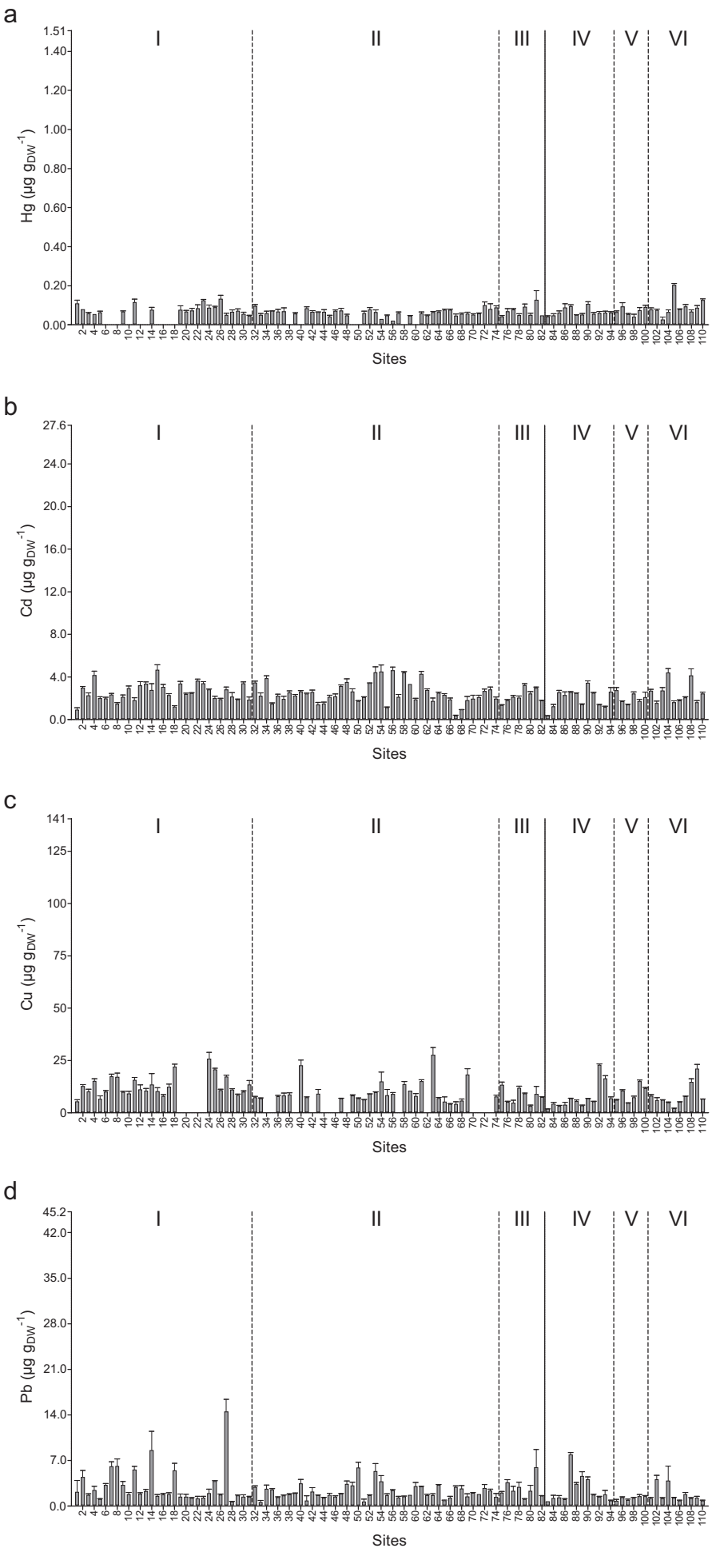
a
I
II
III
IV
V
VI
Hg (µg g$_{DW}^{-1}$)
Sites
b
Cd (µg g$_{DW}^{-1}$)
Sites
c
Cu (µg g$_{DW}^{-1}$)
Sites
d
Pb (µg g$_{DW}^{-1}$)
Sites

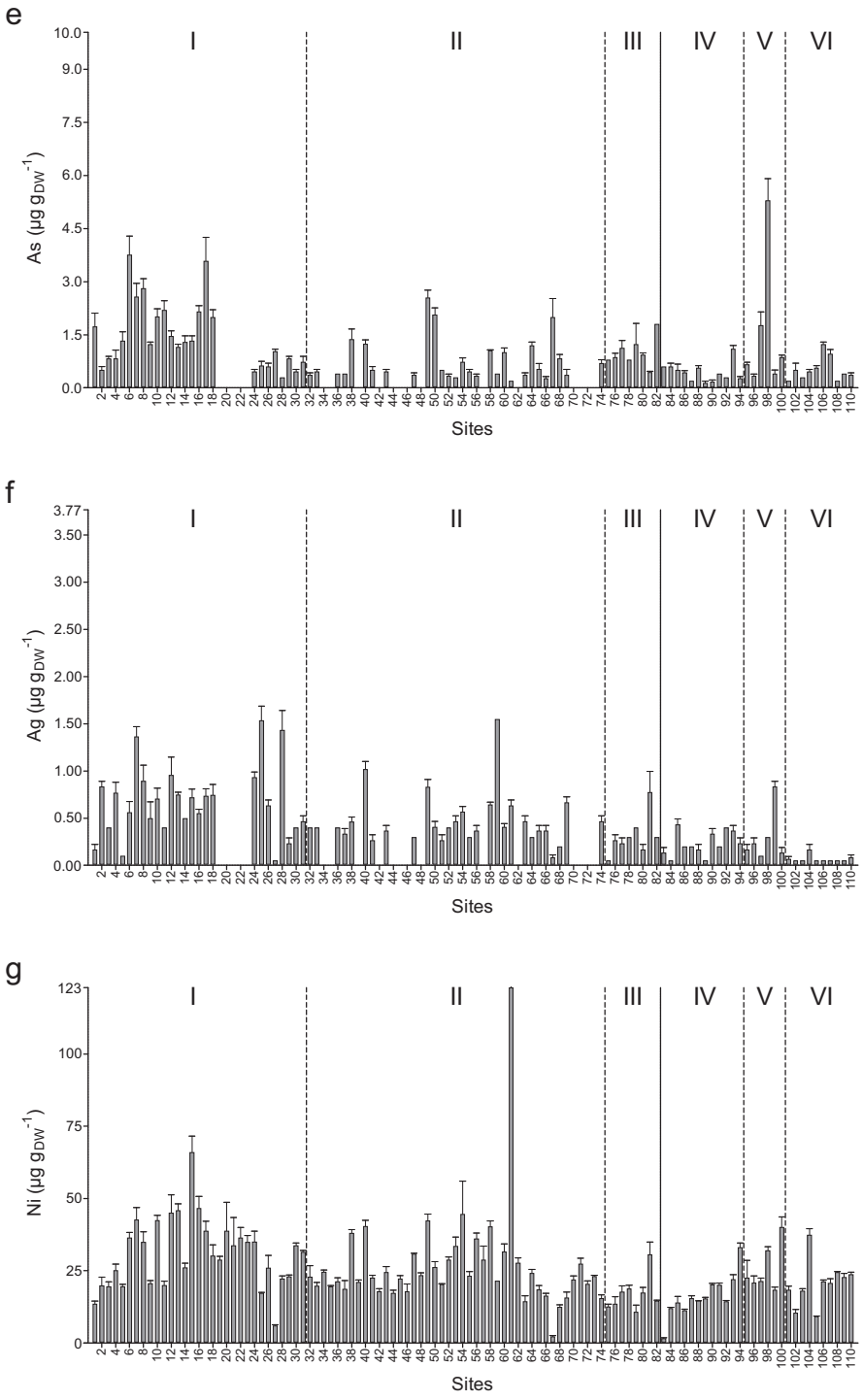

Annex D

a) Hg, b) Cd, c) Cu, d) Pb, e) As, f) Ag and g) Ni concentrations (mean ± SD, in µg g_{DW}^{-1}) measured in the blades of *Posidonia oceanica* adult leaves sampled between April and July of years 2003-2008 in 110 sites (numbers 1-110) located along the coasts of 13 Mediterranean countries. The overall spatial variability of trace element (TE) concentrations is graphically compared by using a proportional ordinate (concentration) scaling between TEs, obtained by multiplying the minimum mean concentration of each TE recorded among the 110 sites by the highest x_{max}/x_{min} mean concentration ratio of 75.3 calculated for Ni (see Table 3). The Mediterranean was subdivided into 6 sub-areas (sub-areas I-VI, separated by dotted vertical lines), according to site location along its north-to-south and west-to-east axes. Sub-area I: European continental coasts; sub-area II: European insular coasts; sub-area III: North African coasts of the western Mediterranean; sub-area IV: western coasts of the eastern Mediterranean; sub-area V: Adriatic coasts; sub-area VI: coasts of the Aegean-Levantine basin. The full vertical line separates sub-areas of the western and the eastern Mediterranean, respectively. For clarity purpose, one in two site number is reported on graphs. Number of replicates n = 3-5, except for Hg in sites 2, 54, 56 (n = 1) and 4 (n = 2) and for Ag, As, Cd, Cu, Ni and Pb in site 59 (n = 2).

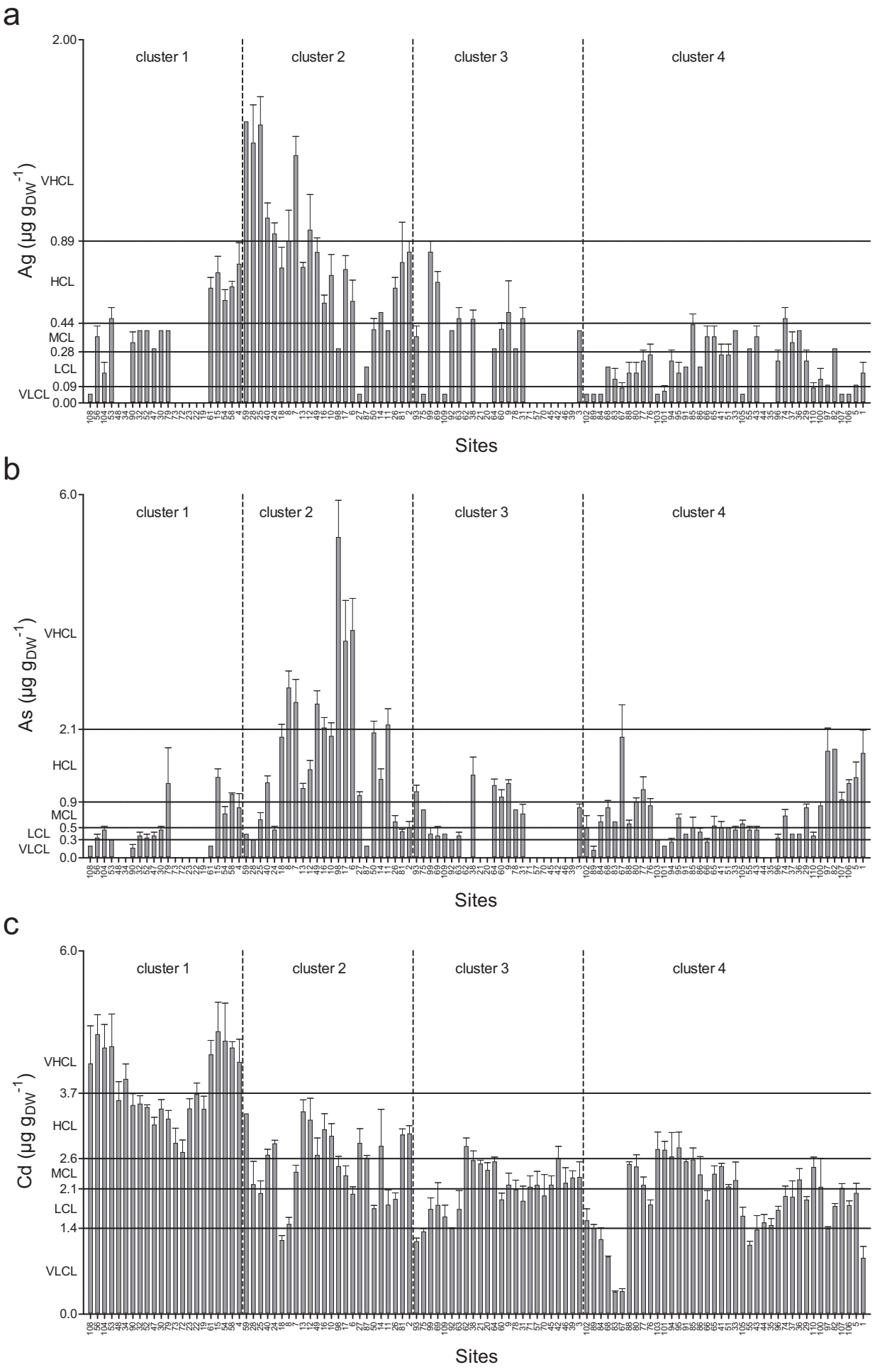
a
cluster 1
cluster 2
cluster 3
cluster 4
Ag (µg g$_{DW}^{-1}$)
VHCL
HCL
MCL
LCL
VLCL
2.00
0.89
0.44
0.28
0.09
0.00
Sites
b
cluster 1
cluster 2
cluster 3
cluster 4
As (µg g$_{DW}^{-1}$)
VHCL
HCL
MCL
LCL
VLCL
6.0
2.1
0.9
0.5
0.3
0.0
Sites
c
cluster 1
cluster 2
cluster 3
cluster 4
Cd (µg g$_{DW}^{-1}$)
VHCL
HCL
MCL
LCL
VLCL
6.0
3.7
2.6
2.1
1.4
0.0
Sites

d

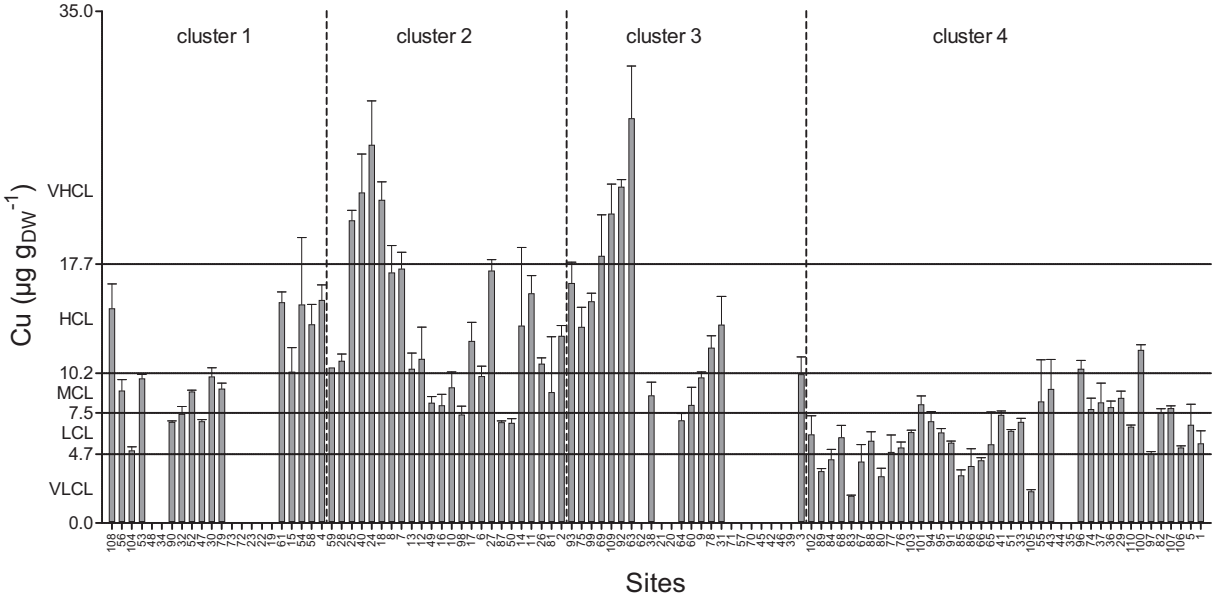
cluster 1
cluster 2
cluster 3
cluster 4
Cu (µg g$_{DW}^{-1}$)
35.0
VHCL
17.7
HCL
10.2
MCL
7.5
LCL
4.7
VLCL
0.0
Sites

e

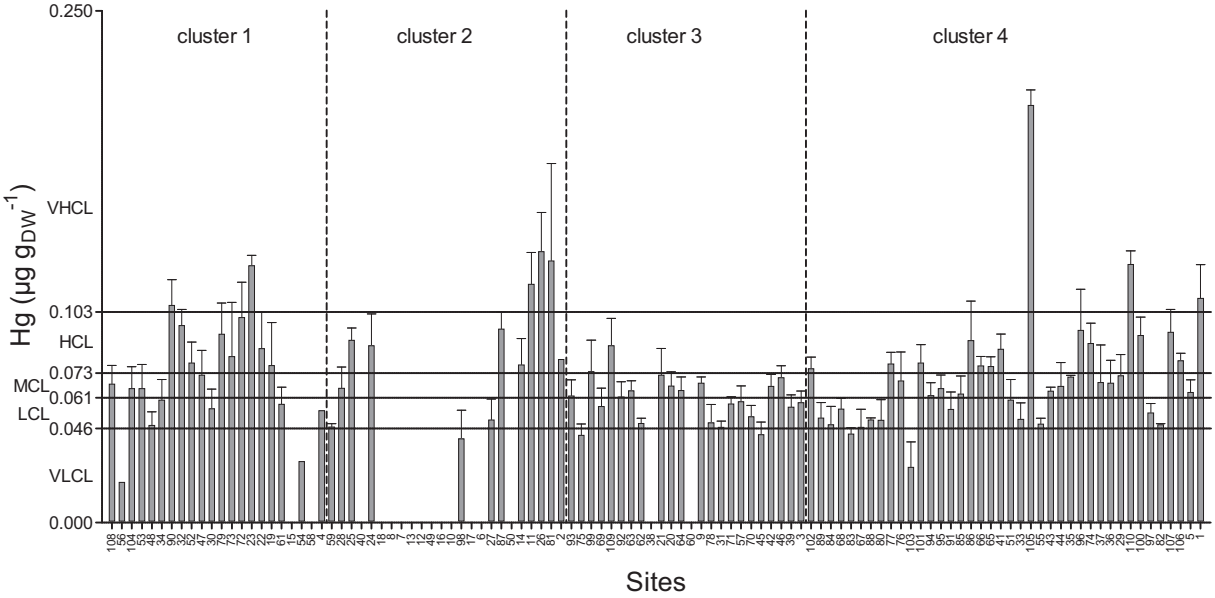
cluster 1
cluster 2
cluster 3
cluster 4
Hg (µg g$_{DW}^{-1}$)
0.250
VHCL
0.103
HCL
0.073
MCL
0.061
LCL
0.046
VLCL
0.000
Sites

f

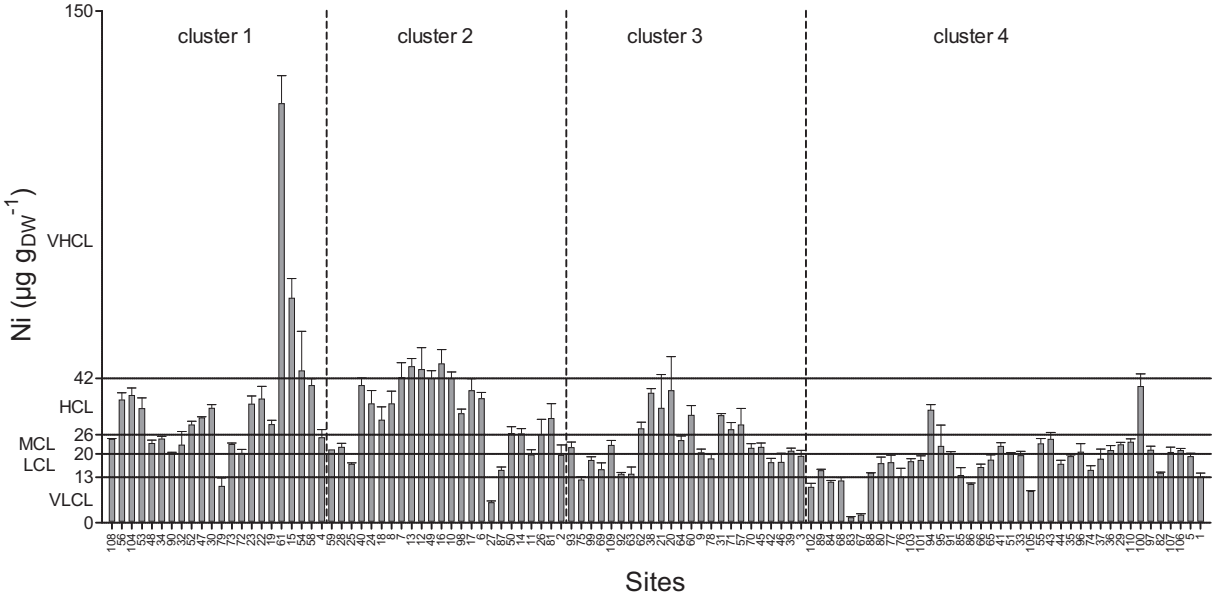
cluster 1
cluster 2
cluster 3
cluster 4
Ni (µg g$_{DW}^{-1}$)
150
VHCL
42
HCL
26
MCL
20
LCL
13
VLCL
0
Sites

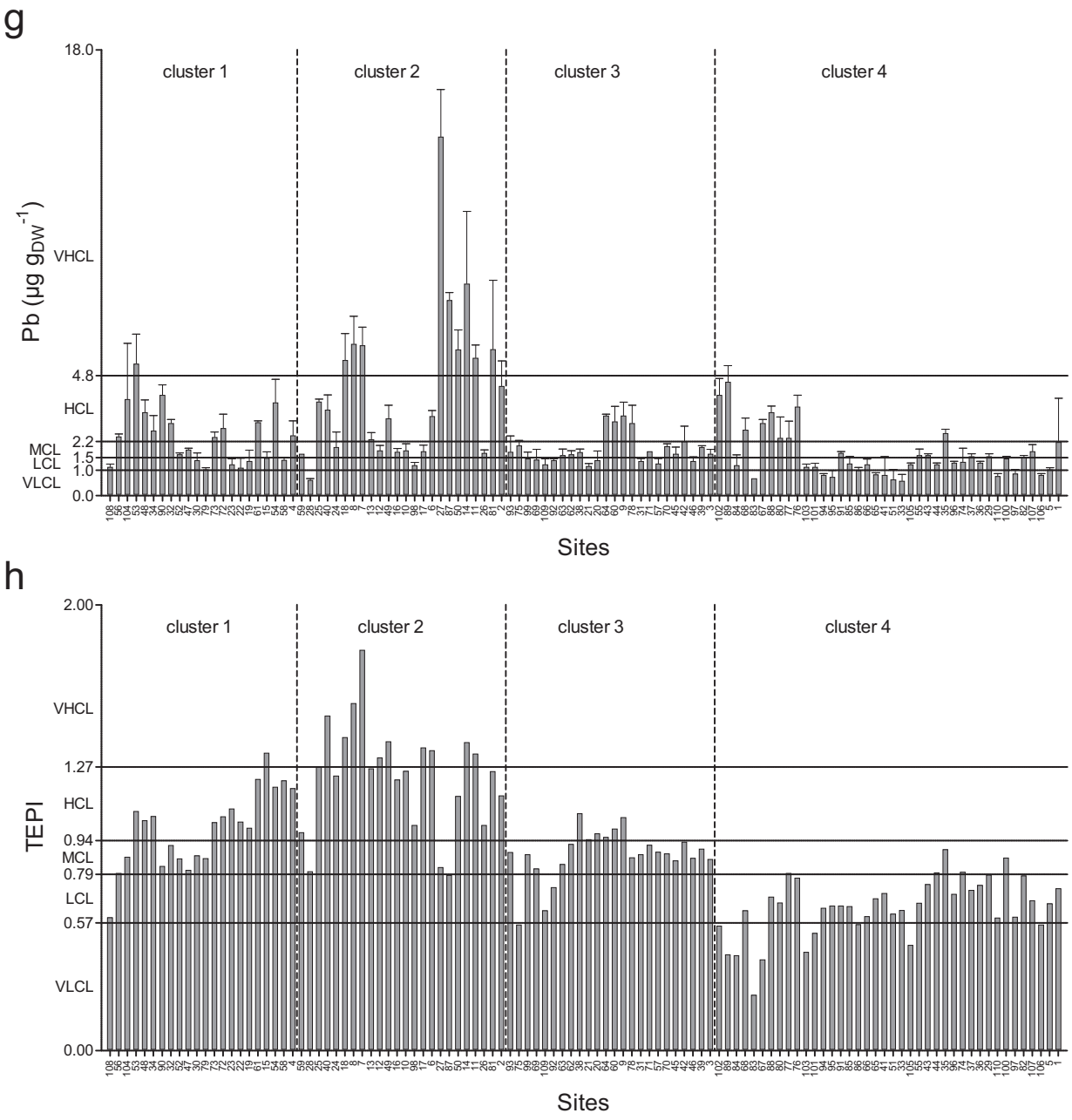

Annex E

a) Ag, b) As, c) Cd, d) Cu, e) Hg, f) Ni and g) Pb concentrations (mean ± SD, in µg g_{DW}^{-1}) measured in the blades of *Posidonia oceanica* adult leaves sampled between April and July of years 2003-2008 in 110 sites (numbers 1-110) located along the coasts of 13 Mediterranean countries, and h) Trace Element Pollution Index (TEPI) values (no unit) calculated from mean normalized trace element (TE) concentrations. Sampling sites are sorted on graphs according to the dendrographic classification after cluster analysis (Euclidean distance as measure of similarity) of TE concentrations and TEPI values. Dotted vertical lines separate the 4 clusters shown on the dendrogram at a linkage distance of 6 (see Fig. 5). TE and TEPI class-limit values (see Table 2) separating sites with contamination levels considered either as very low (VLCL), low (LCL), medium (MCL), high (HCL) or very high (VHCL) are reported on graphs (full horizontal lines).